Prediction of thermal behavior of iSRR-Connector in FRP deck

TU Delft Delft University of Technology

PREDICTION OF THERMAL BEHAVIOR OF iSRR-CONNECTOR IN FRP DECK

by

Haodong QIU

to obtain the degree of Master of Science
in Civil Engineering
Track Structural Engineering
at the Delft University of Technology,

Student number:	5232139
Project duration:	January, 2022 – December, 2022
Thesis committee:	Prof. Marko Pavlović, TU Delft, supervisor
	Can Ayas, TU Delft
	Angeliki Christoforidou, TU Delft

PREFACE

With this thesis project, 'Prediction of thermal behavior of iSRR-Connector in FRP deck', I finished the Master of Science degree in Civil Engineering at the Delft University of Technology. First of all I would like to express gratitude to my supervisor Professor Marko Pavlovic for guidance and encouragement throughout the entire duration of this project. I would like to thank Angeliki Christoforidou, my daily supervisor, for her support and suggestions that helped me a lot. I would like to thank Professor Can Ayas for being a part of my thesis committee.
I am very happy to have completed this interesting research in the last twelve months.I would also like to thank my friends for their company and encouragement during these twelve months. In addition, I would like to thank my dearest friend Luxi especially for helping me do the experiments during her holiday in the hot weathers.

Haodong Qiu
Delft, 2023

ABSTRACT

Hybrid structures consisting of FRP(fiber reinforce polymer) composite decks connected to a steel girder superstructure are gaining more attention by combining the stiffness of steel members with good fatigue endurance and high strength to weight ratio of FRP. However, when composite material FRP is exposed to elevated temperature, delamination and strength reduction could appear due to low transition temperature of fiber and resin. As a result, predicting the temperature of the FRP bridge deck becomes a preliminary requirement for the further study of the FRP bridge deck.

This research is trying to simulate the heat transfer process of the FRP bridge deck and predict the temperature changing process when it is exposed to natural environment. To reach this goal, experiment and FEM(finite element model) are used as main methods. By detecting temperature change history of the FRP bridge deck specimen during hot weathers in Delft, Netherlands, the maximum temperature and heat transfer process of the FRP bridge deck could be studied. On the basis of experimental results, an detailed FEM in Abaqus is built up to simulate the heat transfer process of the specimen used in the experiment. After validating the accuracy of FEM result with experimental data, the FEM is used to predict the temperature of FRP bridge deck that exposed to natural environment in the hottest weather of Netherlands.

In conclusion, the results shows that the temperature of FRP structures could be well predicted which only has 10.5% variance predicting the maximum temperature on the top surface of the specimen and high accuracy of 6% predicting the average temperature of the FRP panels along the thickness. It also has high accuracy of 3.5% predicting the maximum web-core temperature difference. The only insufficient part is that the average temperature difference of web-core has a deviation of 21% with the experimental data. As FRP panels make up the web and flange of the bridge deck which are the main structural parts that bear the stresses, the inaccuracy of predicting temperature of the core is acceptable.

CONTENTS

1

INTRODUCTION

We are living in a rapidly changing world where impossible imaginary becomes reality every day. Before Wright brothers, no one believes that human can fly like birds in the sky, but now flight has become one of the common transportation in people's daily lives. Before 1995, no one believes that fiber could be used to build a bridge, but now vehicles can run on the bridges with FRP (Fiber reinforced polymer) deck.

In recent years, hybrid structures consisting of FRP composite decks connected to a steel girder(s) superstructure are gaining more attention by combining the stiffness of steel members with good fatigue endurance and high strength to weight ratio of FRP [1]. FRP is a composite material consist of polymer and resin. FRP is an orthotropic material which used to be solely applied on aircraft because of its low weight, high performance properties. As for strength in the longitudinal direction, FRP could be 4 times stronger than steel but with only a quarter of steel's density. To compensate for the orthotropic mechanical properties, FRP layers of different directions are put together according to the requirements of the application. So far, the FRP has reached most of the requirements to be an ideal construction material.

Although the research and application of FRP are making progress very fast, there are still several problems remaining to be solved. Firstly, there are limited researches on the behavior of traditional connectors working on FRP decks, thus there is no specific codes explaining how the connector of FRP deck should be designed. Secondly but importantly, the composite material is sensitive to temperature change due to the low glass transition temperature. According to the research, the tensile modulus of some GFRP (glass fiber reinforced polymer) could have reduction up to 60% when temperature reaches 55°C.[2] iSRR-Connector is a novel bolted connector that injected by steel reinforced resin as shown in Figure 1.1. To compensate for the knowledge gap, several experiments have been done to explore the performance of iSRR-Connector. With Gerhard's former studies on static, fatigue and creep performance of iSRR-Connector , the thermal properties of this connector are still not clear[3]. As a result, it is very important to know the temperature within the FRP structure in natural environment and make conservative designs according to the temperature. The main achievement of

1

this thesis is to predict the thermal behavior of the FRP deck with FEM simulation.

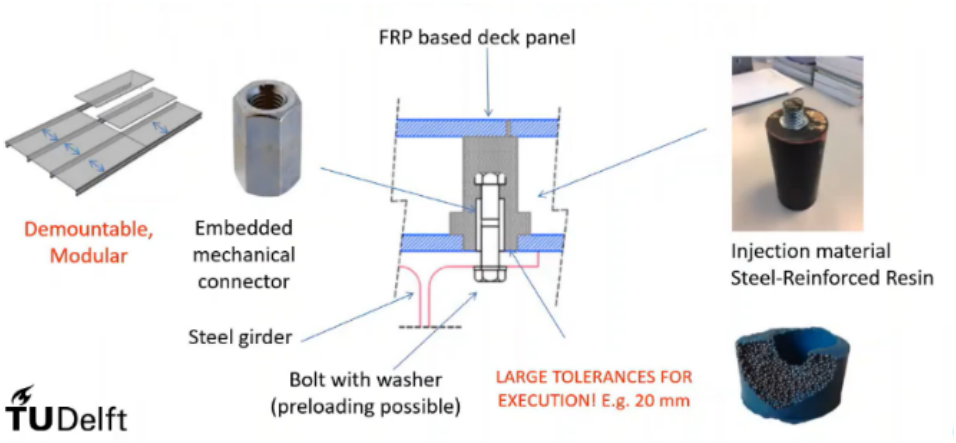

Figure 1.1: iSRR-Connector

1.1. OBJECTIVES

1.1.1. LITERATURE REVIEW

1. **Natural thermal influences on FRP deck.**
   When a bridge deck is exposed to natural environment, it's temperature will be influenced by the ambient environment. It is vital to figure out which factor contributes to the temperature change and how it works, finally getting quantified simulation of the related factors. In this paper, wind convection, solar irradiance, ground reflection, radiation emission are taken into account.

2. **Heat transfer process within FRP deck.**
   To get an accurate simulation of the temperature within FRP deck, the process of heat transfer is important as well. The basic heat transfer process are heat conduction, heat convection and heat radiation. However, it is still not clear that how heat is conducted between different materials within FRP deck or how heat is emitted to the air by convection and radiation.

3. **Methods of building FEM with thermal analysis with FEM software Abaqus.**
   After getting the theoretical knowledge about thermal behavior of the FRP deck, there are still many problems of building finite element model and run thermal analysis with it. For example: how to make detailed model that resembles the real bridge deck, how to set up the interface between different materials and how to set up material properties.

1.1.2. EXPERIMENT

1. **Detect temperature of FRP deck under natural environment.**
   To understand the temperature change process along the whole specimen, the

temperature of top surface and side surface should be detected during the experimental period with specific time interval. The average temperature of top surface and temperature gradient along the vertical side surface offer solid data for further analysis and example for the comparison of the results from FEM simulation.

2. **Record weather data which might influence the temperature of the specimen.**
   As some of the weather factors influence the thermal process of the FRP bridge deck, it is important to find the specific relationships of them. For example, wind speed influences the convection process of the FRP bridge deck. Therefore, specific values of the wind speed at different time is required to find the relationship between wind speed and the convection coefficient. For the same reason, solar irradiance and air temperature are recorded as well.

1.1.3. NUMERICAL MODELING

1. **Detailed modeling of iSRR-Connector.**
   In the Abaqus, the homogenized steel reinforced resin, detailed bolt and nut should be modeled according to the real dimension of the connector.

2. **Modeling of FRP deck.**
   In the Abaqus, the web and core of FRP deck are modeled separately according to the real dimension.

3. **Interfaces, loading and assembly.**
   Assemble different part all together according to the real dimension. Meanwhile, set up interfaces between different parts which simulate the real thermal properties of the contact between different materials. Apply heat influx at top and bottom surface to simulate the solar irradiance and ground reflection as the thermal loading of the FEM.

4. **Modeling of experimental situation.**
   Define different convection coefficient according to the wind speed, air temperature from the experiment. Define different sink temperature for the heat emission process according to different air temperature from the experiment. Define different value of the heat flux according to the solar irradiance from experiment.

5. **Running simulations at different environmental situations.**
   Run simulations according to different experimental data with different convection, heat fluxes and radiations.

6. **Validation and discussion of FEM results.**
   Compare the FEM result and the experimental result with the same weather data, validating the accuracy of the FEM. Furthermore, methods and material properties will be discussed to increase the accuracy of the model.

7. **Predicting the thermal behavior for the hottest day in the Netherlands.**
   Input the weather data of the hottest day in the Netherlands, predicting the

temperature changing procedure of the FRP bridge deck if it is exposed to the sun light in natural environment.

1.2. CHALLENGES

1. **What kind of thermal properties is the FRP deck and steel reinforced resin?**
   Steel reinforced resin is an composite material which is composed of steel particles and resin. As no one has detected its thermal properties before, the thermal properties of this composite material should be decided by ourselves according to the existing data.

2. **How are the thermal properties of FRP influenced by the change of temperature?**
   FRP is a composite material which has low transition temperature and suffers from delamination. How will the thermal properties of the FRP change with temperature needs to be studied.

3. **How to set up a detailed Abaqus model of FRP deck with iSRR-connector accurately built inside?**
   As there is no such kind of finite element model before, it is not clear how detailed the FEM should be to have a high accuracy prediction of the temperature of the FRP bridge deck.

4. **How to simulate the natural environmental influences to make simulation results accurately predict for real situations?**
   The natural environmental factors influence the thermal process of the bridge deck in complicated ways. Not only versatile thermal processes should be taken into account but these thermal process are different on different materials as well.

2

THERMAL PROPERTIES AND ENVIRONMENTAL INFLUENCES

In this chapter, the structure of FRP deck, the theory of heat transfer, the thermal properties of materials will be introduced. Firstly, the structure and composition of the FRP deck will be introduced. Secondly, knowing the basic theory of heat transfer helps with the set up of FEM (finite element model). Thirdly, the properties of the materials and the input of environmental thermal influences could increase the accuracy of the FEM simulation.

2.1. STRUCTURE OF FRP DECK

The FRP deck discussed in this thesis is sandwich panel produced by vaccum infusion method which is mainly made up of FRP flange, FRP web and foam cores. The FRP flange and web are set as "I" shape, in which the flange bears tensile and compression stress while the web bears shear stress.

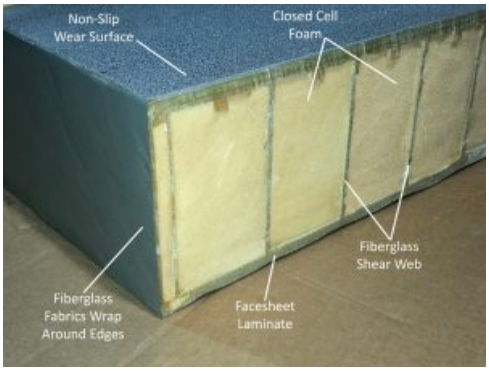

Figure 2.1: Cross-section of FRP deck

The plan view and section view of the FRP deck are shown as Figure2.2 and Figure2.3:

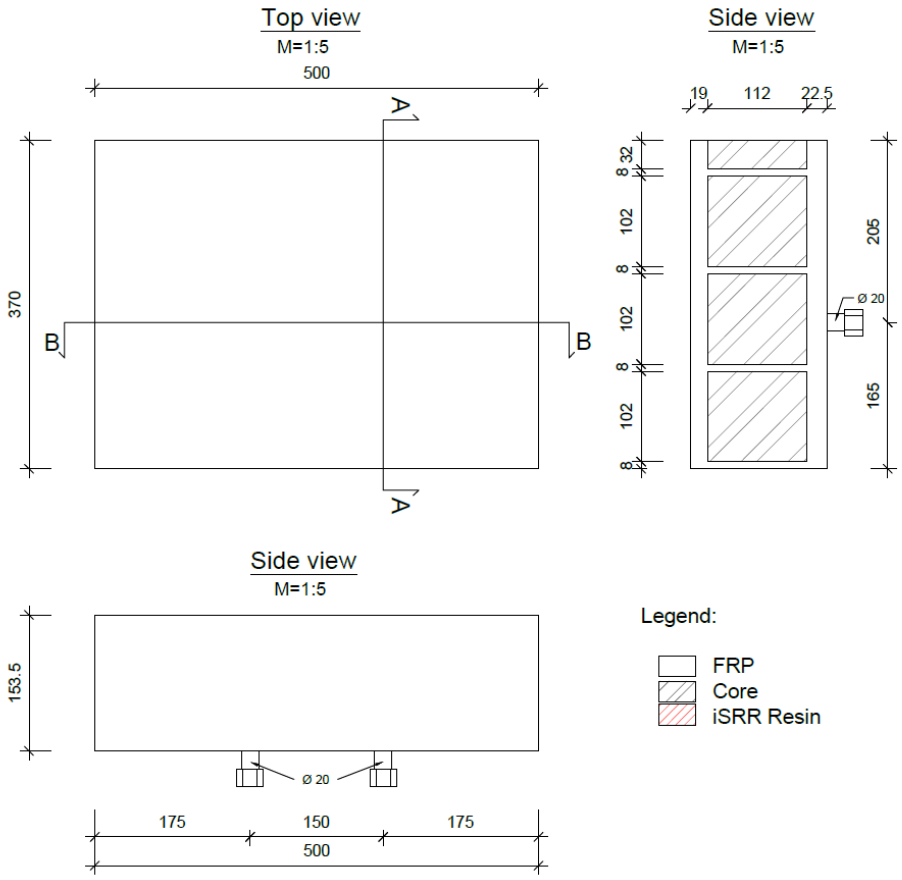

Figure 2.2: Plan view of the FRP deck

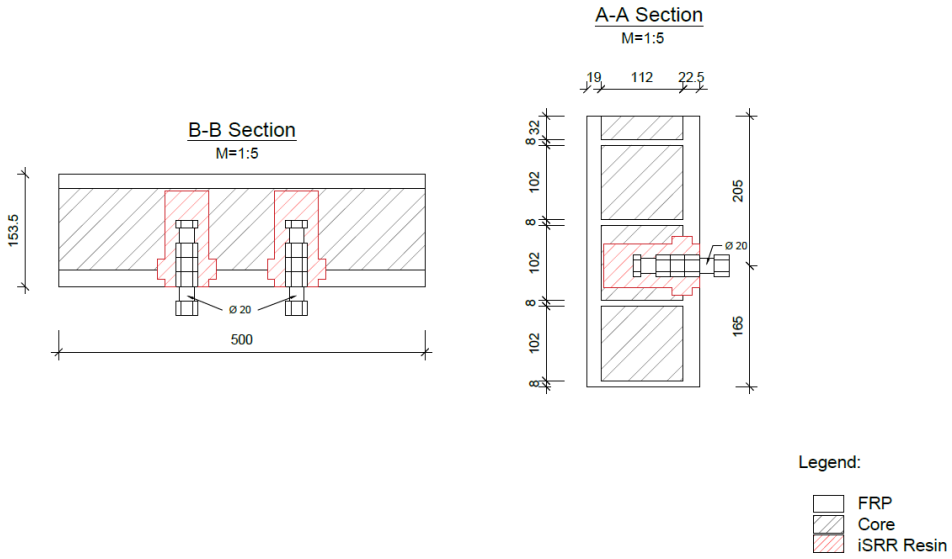

Figure 2.3: Section view of the FRP deck

2.2. BASICS OF HEAT TRANSFER

In general, heat transfer describes the flow of heat (thermal energy) due to temperature differences and the subsequent temperature distribution and changes.

The study of transport phenomena concerns the exchange of momentum, energy, and mass in the form of conduction, convection, and radiation. These processes can be described via mathematical formulas.

2.3. THEORY OF CONDUCTION

Conduction is the mode of heat transfer in which energy exchange takes place in solids or in fluids in rest from the region of high temperature to the region of low temperature due to the presence of temperature gradient in the body.[4] The Fourier's Law states that heat flux (q resulting from thermal conduction is directly proportional to the magnitude of the temperature gradient.The constant of proportionality is described by the constant k.[5]

$$q = -k\frac{dT}{dx} \tag{2.1}$$

The constant, k, is called the thermal conductivity with the dimensions of $\frac{W}{m*K}$.
In the FRP deck model, the heat transfer method within the deck is mainly conduction, thus the k (thermal conductivity) values of all the materials are essential.

2.4. THEORY OF RADIATION

Energy radiates from all types of matter under all conditions and at all times. The emission of thermal radiation arises from random fluctuations in the quantized internal energy states of the emitting matter. Temperature is a measure of the internal energy level of matter, and the nature of the fluctuations can be related to an object's temperature. Once the energy is radiated, it propagates as an electromagnetic (EM) wave. If the waves encounter matter, they may partially lose their energy and increase the internal energy of the receiving matter. This is called absorption. The amount of emitted and absorbed radiation are functions of the physical and chemical properties of the material as well as its internal energy level, as quantified by its temperature.[6]

In other words,A body that can emit radiation $(\dot{Q}_E)$ can also reflect $(\dot{Q}_R)$, transmit $(\dot{Q}_T)$, and absorb $(\dot{Q}_A)$ the falling radiation.

$$\begin{aligned} \dot{Q} &= \dot{Q}_A + \dot{Q}_T + \dot{Q}_R \\ 1 &= \frac{\dot{Q}_A}{\dot{Q}} + \frac{\dot{Q}_T}{\dot{Q}} + \frac{\dot{Q}_R}{\dot{Q}} \\ 1 &= \alpha^S + \tau^S + \rho^S \end{aligned} \tag{2.2}$$

where

α^S : Absorptance

τ^S : Transmittance

ρ^S : Reflectance

Different materials are classified according to their radiation characteristics as Black body, Gray body, White body, Opaque body and Transparent body. In this thesis the **Black body** is used for all objects, which absorbs all incoming radiation and emits energy of a characteristic, temperature-dependent spectrum:

Black Body: $\alpha^S = 1 \quad \rho^S = 0 \quad \tau^S = 0$

Stefan-Boltzmann law: The thermal energy radiated by a black body radiator per second per unit area is proportional to the fourth power of the absolute temperature and is given by:

$$\frac{P}{A} = \sigma T^4 \tag{2.3}$$

where σ is the Stefan-Boltzmann constant which can be derived from other constants of nature:

$$\sigma = \frac{2\pi^5 k^4}{15c^2h^3} = 5.670373 * 10^{-8} W m^{-2} K^{-4}$$

For hot objects other than ideal radiators, the law is expressed in the form:

$$\frac{P}{A} = e\sigma T^4 \tag{2.4}$$

where e is the emissivity of the object ($e = 1$ for ideal radiator). If the hot object is radiating energy to its colder surroundings at temperature T_c, the net rate takes the form:

$$P = e\sigma A\left(T^4 - T_c^4\right) \tag{2.5}$$

2.5. THEORY OF CONVECTION

Convective heat transfer, or simply, convection, is the study of heat transport processes effected by the flow of fluids.[7]

Convection can be divided into **forced convection**, **natural convection** and **mixed convection** depending on how the fluid motion is initiated. Natural convection is caused for instance by buoyancy effects (warm fluid rises and cold fluid falls due to density difference). In the other case, forced convection causes the fluid to move by external means such as a fan, wind etc. Mixed convection is the combination of forced convection and natural convection.

2.5.1. FORCED CONVECTION

[8] Convection heat transfer is complicated since it involves fluid motion as well as heat conduction. The fluid motion enhances heat transfer (the higher the velocity the higher the heat transfer rate). The rate of convection heat transfer is expressed by Newton's law of cooling:

$$\begin{aligned} q^{\bullet}_{\text{conV}} &= h\left(T_s - T_\infty\right) \quad \left(W/m^2\right) \\ Q^{\bullet}_{conv} &= hA\left(T_s - T_\infty\right) \quad (W) \end{aligned} \tag{2.6}$$

The convective heat transfer coefficient h strongly depends on the fluid properties and roughness of the solid surface, and the type of the fluid flow (laminar or turbulent).

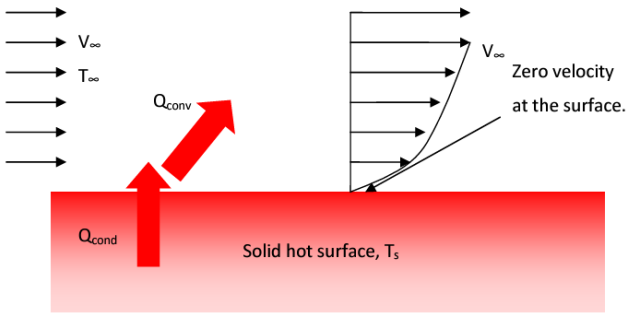

Figure 2.4: Forced convection

It is assumed that the velocity of the fluid is zero at the wall (no-slip) condition. As a result, it is pure conduction when heat transfer from solid surface to the fluid layer adjacent to the surface.

$$\left.\begin{aligned} \dot{q_{\text{conv}}} = \dot{q_{\text{cond}}} = -\ k_{\text{fluid}} \left.\frac{\partial T}{\partial y}\right|_{y=0} \end{aligned}\right\} \rightarrow h = \frac{-\ k_{\text{fluid}} \left.\frac{\partial T}{\partial y}\right|_{y=0}}{T_s - T_\infty} \quad \left(W/m^2.K\right) \tag{2.7}$$

$$\dot{q}_{conv} = h\left(T_s - T_\infty\right)$$

The convection coefficient h varies along the flow direction. The average convection coefficient is determined by properly averaging the local heat transfer coefficient over teh entire surface.

VELOCITY BOUNDARY LAYER

As there is friction between fluid layers, the fluid velocity U_∞ remains unchanged at velocity boundary layer. And the friction between two adjacent layers can be described as:

$$\tau_s = \mu \left.\frac{\partial V}{\partial y}\right|_{y=0} \quad \left(N/m^2\right) \tag{2.8}$$

where μ is the dynamic viscosity of the fluid $\mathrm{kg/m \cdot s}$ or $\mathrm{N \cdot s/m^2}$.

Viscosity is a measure of fluid resistance to flow, and is a strong function of temperature.

NON-DIMENSIONAL GROUPS

In convection, it is a common practice to non-dimensionalize the governing equations and combine the variables which group together into dimensionless numbers (groups).

Nusselt number: non-dimensional heat transfer coefficient

$$Nu = \frac{h\delta}{k} = \frac{q^{\bullet}_{\text{conv}}}{q^{\bullet}_{\text{cond}}} \tag{2.9}$$

where δ is the characteristic length, i.e. D for the tube and L for the flat plate. Nusselt number represents the enhancement of heat transfer through a fluid as a result of convection relative to conduction across the same fluid layer.

Reynolds number: ratio of inertia forces to viscous forces in the fluid

$$\mathrm{Re} = \frac{\text{inertia forces}}{\text{viscous forces}} = \frac{\rho V \delta}{\mu} = \frac{V\delta}{\nu} \tag{2.10}$$

Re number at which the flow becomes turbulent is called the critical $Reynoldsnumber$. For flat plate the critical Re is determined by experiments, approximately $Re\ criticle = 5 * 10^5$.

The Reynolds number at which the flow becomes turbulent is called the critical Reynolds number. For flat plate the critical Re is experimentally determined to be approximately Re critical $= 5 \times 10^5$.

Prandtl number: is a measure of relative thickness of the velocity and thermal boundary layer

$$\mathrm{Pr} = \frac{\text{molecular diffusivity of momentum}}{\text{molecular diffusivity of heat}} = \frac{\nu}{\alpha} = \frac{\mu C_p}{k} \tag{2.11}$$

where fluid properties are:
mass density : $\rho, (\mathrm{kg/m^3})$ specific heat capacity : $C_p, (J/\mathrm{kg}\cdot\mathrm{K})$
dynamic viscosity : $\mu, (N\cdot s/m^2)$ kinematic viscosity : $\nu, \mu/\rho\,(\mathrm{m^2/s})$
thermal conductivity : $k, (W/m\cdot K)$ thermal diffusivity : $\alpha, k/(\rho\cdot C_p)\,(m^2/s)$
Velocity: $V, (m/s)$

FLOW OVER FLAT PLATE

The friction and heat transfer coefficient for a flat plate can be determined by solving the conservation of mass, momentum, and energy equations (either approximately or numerically). They can also be measured experimentally. It is found that the Nusselt number can be expressed as:

$$Nu = \frac{hL}{k} = C\,\mathrm{Re}_L^m\,\mathrm{Pr}^n \tag{2.12}$$

where C, m, and n are constants and L is the length of the flat plate. The properties of the fluid are usually evaluated at the film temperature defined as:

$$T_f = \frac{T_s + T_\infty}{2} \tag{2.13}$$

LAMINAR FLOW

The local friction coefficient and the Nusselt number at the location x for laminar flow over a flat plate are

$$\begin{aligned} Nu_x &= \frac{hx}{k} = 0.332\,\mathrm{Re}_x^{1/2}\,\mathrm{Pr}^{1/3} \quad \mathrm{Pr} \geq 0.6 \\ C_{f,x} &= \frac{0.664}{\mathrm{Re}_x^{1/2}} \end{aligned} \tag{2.14}$$

where x is the distant from the leading edge of the plate and $Re_x = \rho V_\infty x/\mu$. The averaged friction coefficient and the Nusselt number over the entire isothermal plate for laminar regime are:

$$\begin{aligned} Nu &= \frac{hL}{k} = 0.664\,\mathrm{Re}_L^{1/2}\,\mathrm{Pr}^{1/3} \quad \mathrm{Pr} \geq 0.6 \\ C_f &= \frac{1.328}{\mathrm{Re}_L^{1/2}} \end{aligned} \tag{2.15}$$

Taking the critical Reynolds number to be 5×10^5, the length of the plate x_{cr} over which the flow is laminar can be determined from

$$\mathrm{Re}_{cr} = 5\times10^5 = \frac{V_\infty X_{cr}}{\nu} \tag{2.16}$$

TURBULENT FLOW

The local friction coefficient and the Nusselt number at location x for turbulent flow over a flat isothermal plate are:

$$\begin{aligned} Nu_x &= \frac{hx}{k} = 0.0296\,\mathrm{Re}_x^{4/5}\,\mathrm{Pr}^{1/3} \quad 0.6 \leq \mathrm{Pr} \leq 60 \quad 5\times10^5 \leq \mathrm{Re}_x \leq 10^7 \\ C_{f,x} &= \frac{0.0592}{\mathrm{Re}_x^{1/5}} \quad 5\times10^5 \leq \mathrm{Re}_x \leq 10^7 \end{aligned} \tag{2.17}$$

The averaged friction coefficient and Nusselt number over the isothermal plate in turbulent region are:

$$\begin{aligned} Nu &= \frac{hL}{k} = 0.037\,\mathrm{Re}_x^{4/5}\,\mathrm{Pr}^{1/3} \quad 0.6 \le \mathrm{Pr} \le 60 \quad 5\times10^5 \le \mathrm{Re}_L \le 10^7 \\ C_f &= \frac{0.074}{\mathrm{Re}_L^{1/5}} \quad 5\times10^5 \le \mathrm{Re}_L \le 10^7 \end{aligned} \tag{2.18}$$

COMBINED LAMINAR AND TURBULENT FLOW

If the plate is sufficiently long for the flow to become turbulent (and not long enough to disregard the laminar flow region), we should use the average values for friction coefficient and the Nusselt number.

$$\begin{aligned} C_f &= \frac{1}{L}\left(\int_0^{x_c} C_{f,x,\,\text{Lamin ar}}\,dx + \int_{x_{cr}}^{L} C_{f,x,\,\text{Turbulent}}\,dx\right) \\ h &= \frac{1}{L}\left(\int_0^{x_{cr}} h_{x,\,\text{La min ar}}\,dx + \int_{x_{cr}}^{L} h_{,x,\,\text{Turbulent}}\,dx\right) \end{aligned} \tag{2.19}$$

where the critical Reynolds number is assumed to be 5×10^5. After performing the integrals and simplifications, one obtains:

$$\begin{aligned} Nu &= \frac{hL}{k} = \left(0.037\,\mathrm{Re}_x^{4/5} - 871\right)\mathrm{Pr}^{1/3} \quad 0.6 \le \mathrm{Pr} \le 60 \quad 5\times10^5 \le \mathrm{Re}_L \le 10^7 \\ C_f &= \frac{0.074}{\mathrm{Re}_L^{1/5}} - \frac{1742}{\mathrm{Re}_L} \quad 5\times10^5 \le \mathrm{Re}_L \le 10^7 \end{aligned} \tag{2.20}$$

2.5.2. NATURAL CONVECTION

MECHANISMS OF NATURAL CONVECTION

Consider a hot object exposed to cold air. The temperature of the outside of the object will drop because of heat transfer with cold air , and the temperature of adjacent air to the object will rise. Consequently, the object is surrounded with a thin layer of warmer air and heat will be transferred from this layer to the outer layers of air.[9]

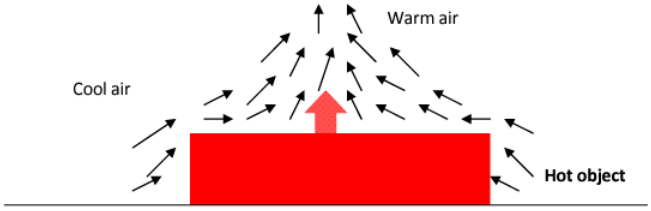

Figure 2.5: Natural convection

The density of the air adjacent to the hot object is lower due to higher temperature. As a result, the heated air rises. This movement is called the natural convection current.

When this object is put in a gravitational field, there is a net force pushing the light fluid upward in the heavier fluid. This force is called boyancy force. The magnitude of the buoyancy force is the weight of the fluid displaced by the body.

$$\mathrm{F_{buoyancy}} = \rho_{\mathrm{fluid}}\, \mathrm{gV_{body}} \tag{2.21}$$

where V_{body} is the volume of the portion of the body immersed in the fluid. The net force is:

$$\begin{aligned} F_{\mathrm{net}} &= W - F_{\mathrm{buoyancy}} \\ F_{\mathrm{net}} &= \left(\rho_{\mathrm{body}} - \rho_{\mathrm{fluid}}\right) g V_{\mathrm{body}} \end{aligned} \tag{2.22}$$

Density is a function of temperature, the variation of density of a fluid with temperature at constant pressure can be expressed in terms of the volume expansion coefficient β, defined as:

$$\begin{aligned} \beta &= -\frac{1}{\rho}\left(\frac{\partial \rho}{\partial T}\right)_p \left(\frac{1}{K}\right) \\ \beta &\approx -\frac{1}{\rho}\frac{\Delta \rho}{\Delta T} \rightarrow \Delta \rho \approx -\rho \beta \Delta T \quad \text{at constantP} \end{aligned} \tag{2.23}$$

It can be shown that for an ideal gas

$$\beta_{\text{ideal gas}} = \frac{1}{T} \tag{2.24}$$

where T is the absolute temperature. Note that the parameter $\beta \Delta T$ represents the fraction of volume change of a fluid that corresponds to a temperature change ΔT at constant pressure.

GRASHOF NUMBER

Grashof number is a dimensionless group, which represents the ratio of the buoyancy force to the viscous force acting on the fluid, and it can be expressed as:

$$Gr = \frac{g\beta\left(T_s - T_\infty\right)\delta^3}{\upsilon^2} \tag{2.25}$$

where
g = gravitational acceleration, $\mathrm{m/s^2}$
β = coefficient of volume expansion, $1/K$
δ = characteristic length of the geometry (area over perimeter), m
υ = kinematics viscosity of the fluid, $\mathrm{m^2/s}$

NATURAL CONVECTION CORRELATIONS

The complexities of the fluid flow make it very difficult to obtain simple analytical relations for natural convection. Thus, most of the relationships in natural convection are based on experimental correlations. The Rayleigh number is defined as the product of the Grashof and Prandtl numbers:

$$Ra = G_r\,\mathrm{Pr} = \frac{g\beta\left(T_s - T_\infty\right)\delta^3}{\upsilon^2}\,\mathrm{Pr} \tag{2.26}$$

The Nusselt number in natural convection is in the following form:

$$Nu = \frac{h\delta}{k} = CRa^n \tag{2.27}$$

where the constants C and n depend on the geometry of the surface and the flow. These relationships are for isothermal surfaces

ISOTHERMAL VERTICAL PLATE

For a vertical plate, the characteristic length is L.

$$Nu = \begin{cases} 0.59Ra^{1/4} & 10^4 < Ra < 10^9 \\ 0.1Ra^{1/3} & 10^9 < Ra < 10^{13} \end{cases} \tag{2.28}$$

ISOTHERMAL HORIZONTAL PLATE

The characteristics length is A/p where the surface area is A, and perimeter is p.
a) Upper surface of a hot plate

$$Nu = \begin{cases} 0.54\mathrm{Ra}^{1/4} & 10^4 < Ra < 10^7 \\ 0.15\mathrm{Ra}^{1/3} & 10^7 < Ra < 10^{11} \end{cases} \tag{2.29}$$

b) Lower surface of a hot plate

$$Nu = 0.27\mathrm{Ra}^{1/4} \quad 10^5 < Ra < 10^{11} \tag{2.30}$$

2.6. THERMAL PROPERTIES AND METEOROLOGICAL DATA

2.6.1. CONDUCTION AND RADIATION

According to the equation 2.1 and equation 2.5, conductivity and emissivity of the material could express the processes of conduction and radiation. The specific heat is the heat required to raise the temperature of the unit mass of a given substance by a given amount. As for the composite material iSRR inside the connector which is made of steel particles and resin, the properties are calculated proportionally to the volume of steel(0.8) and resin(0.2). The thermal properties of steel is the average value of steel with different carbon contents[10]. The thermal properties of CFRP(Carbon fiber reinforced polymer) are got from the indicative thermal properties for carbon-epoxy composite (mass volume fraction=72%) in "Design of fibre-polymer composite structures". The thermal properties of foam are got from the the foam producer "Kingspan"[11].

Table 2.1: Material thermal properties

Material	Conductivity(W/mK)	Emissivity	Specific heat(J/Kg)	Density(g/mm^3)
Steel	45.00	0.85	0.466	0.00785
CFRP(Carbon)	1.36	0.9	1.287	0.00160
Resin(epoxy)	0.20	0.80	1.111	0.00100
iSRR	36.04	0.84	0.595	0.00648
Foam	0.02	0.60	1.470	0.00006

2.6.2. CONVECTION

THERMAL PROPERTIES OF AIR

In the convection model, the fluid around the hot surface is air, the table2.2 show the thermal properties of air.[12][13]

Table 2.2: Thermal properties of air

Thermal expansion coefficient $\beta, \times 10^{-3} k^{-1}$	3.4
Specific heat C_p, $(J/\mathrm{kg}\cdot\mathrm{K})$	1007
Thermal conductivity k, $(W/m\cdot K)$	0.0255
Dynamic viscosity μ, $\left(N\cdot s/m^2\right)$	1.85×10^{-5}
Kinematic viscosity v, $(\mathrm{m}^2/\mathrm{s})$	1.56×10^{-5}

CONVECTION TYPES

As the FEM is built up in the Abaqus software, the film function is used to represent the convection process. In the definition of film properties for heat transfer, the film coefficient and sink temperature are the parameters that should be defined manually.The sink temperature is just the ambient temperature, the film coefficient is the convection coefficient defined in equation2.12 and equation2.27.

However, there is still problems deciding the convection coefficient in natural environment because the air movement in real world is not simply forced convection or natural convection mentioned in section2.5. Mixed convection problems are characterized by the Grashof number (for the natural convection) and the Reynolds number (for the forced convection). The relative effect of buoyancy on mixed convection can be expressed through the Richardson number Ri[14]:

$$\begin{aligned} Ri &< 0.01 && \textbf{Forced convection} \\ 0.01 < Ri &< 100 && \textbf{Mixed convection} \\ Ri &> 100 && \textbf{Natural convection} \end{aligned} \tag{2.31}$$

$Where \quad Ri = Gr/Re^2$[15]

As the Re changes along with the length of the plate, $Re_{0.5L}$ at $0.5L$ is used as the average number for the equation. As wind in natural environment comes from random directions, all the length L used here is the characteristic length of the horizontal surface of the specimen:

$$L = \frac{A}{P} = 0.106 \quad m \tag{2.32}$$

Where
A is the area of the convection surface
P is the perimeter of the convection surface

FORCED CONVECTION

The assumption for a forced flow is acceptable when $Ri << 1$, where buoyancy is low and the inertia large which means high speed wind controls the flow.

According to the dimension of the specimen and equation2.16, X_{cr} is $0.9m$ when maximum wind speed is $10m/s$, which is bigger than the characteristic length of the specimen ($0.106m$). And the forced convection is all considered as laminar flow in this thesis, the convection coefficient as following:

$$h = \frac{0.664\,\mathrm{Re}_L^{1/2}\,\mathrm{Pr}^{1/3}\,\mathrm{k}}{L} \quad \mathrm{Pr} \geq 0.6 \tag{2.33}$$

NATURAL CONVECTION

The natural convection is the main heat-transport mechanism when $Ri >> 1$. Two categories of natural convection is distinguished in our case: hot surface facing top and hot surface facing bottom. Because the top surface is subjected to sun light directly and exposed more to wind than bottom surface, here we only calculate the hot surface facing top category and set the convection coefficient of bottom surface at half value of the top surface according to the equation2.29 and equation2.30

The convection coefficient is calculated according to the equation2.27.

$$\begin{aligned} h_{top} &= \frac{CRa^n k}{L} \\ h_{bot} &= \frac{1}{2} h_{top} \end{aligned} \tag{2.34}$$

Where the c and n value could be decided according to Incropera's (first row)[16] and Goldstein's (the other rows)[17] experimental results.

Table 2.3: Coefficient c and n for equation2.34

Region of Rayleigh number Ra	c	n
$10^4 \leq Ra \leq 10^7$	0.54	0.25
$2 \cdot 10^3 \leq Ra \leq 10^4$	0.38	0.25
$10 \leq Ra \leq 2 \cdot 10^3$	0.467	0.2

MIXED CONVECTION

The mixed convection is calculated as a combination of forced convection and natural convection[15].

$$\begin{aligned} Nu^{7/2} &= Nu_{\text{forced}}^{7/2} + Nu_{\text{Natural}}^{7/2} \\ h &= \frac{Nu \cdot k}{L} \end{aligned} \tag{2.35}$$

To be concluded, the Matlab script could be found in Appendix A.

METEOROLOGICAL DATA

As radiation, convection are both influenced by the temperature difference between surface and ambient air, the ambient temperature data is quite important. For the calculation of convection, wind speed is also needed. Limited by the equipment and time, these data are got from measurements from the Royal Netherlands Meteorological Institute (KNMI)[18].

3

METHOD

Firstly, to achieve the goal of predicting the thermal behavior of FRP bridge deck in natural environment, an accurate FEM model is required. In this thesis the Abaqus CAE software is used to build up the FEM model with the thermal properties got in chapter2. Furthermore, the result of the FEM simulation will be validated by experiment result with the same dimension.

3.1. FINITE ELEMENT MODEL

In Abaqus software, the process of building a FEM is like following:

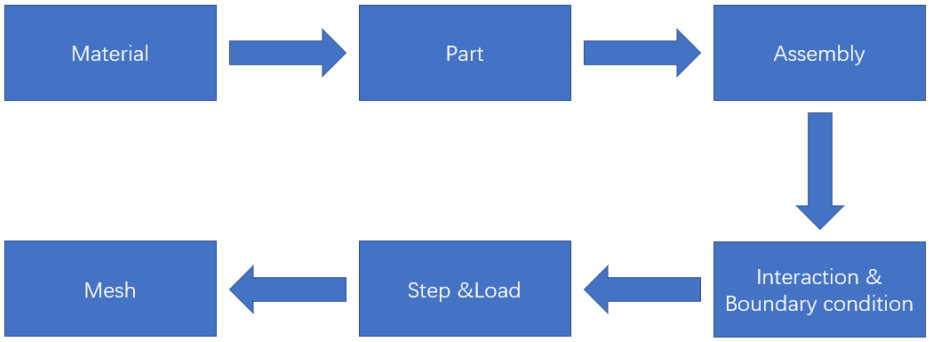

Figure 3.1: Process of building FEM

3.1.1. MATERIAL

First of all, the heat transfer analysis need to input Stefan-Boltzmann constant as $5.67 \times 10^{-14} \quad W \cdot mm^{-2} \cdot K^{-4}$.
There are 4 materials used in the FEM: foam, steel, GFRP, iSRR, and they are defined for density, thermal conductivity, specific heat and emissivity.
As the properties of the materials used in the experiment is not accessible, the value maybe adjusted in later simulations according to the experimental results.

FOAM

Polyurethane foam is a insulating material with a large number of gas-filled pockets which prevent large-scale convection. The typical thermal conductivity of foam is between 0.02 and $0.035 W/m \cdot K$[19], of which the value of $0.02 W/m \cdot K$ is taken.
The typical density of foam is between 24 to $300 kg/m^3$[20], which has a large scale of values. According to the foam density in Matthew's FRP deck which varies from 30 to $90 kg/m^3$[21], finally the value of $60 kg/m^3$ is taken in our thesis.
The emissivity of foam is about 0.6[22] and specific heat of foam is about $1.47 J/Kg$[23].

STEEL

Steel has a conductivity of $45 W/mK$[10], specific heat of $0.466 J/Kg$[24], density of $0.00785 g/mm^3$[25], emissivity of 0.85[12].

GFRP

GFRP is a composite material consisted of resin and glass fiber, which has conductivity of $0.8 W/mK$, specific heat of $0.837 J/gK$, density of $0.0025 g/mm^3$, emissivity of 0.84.
When the temperature increases, the thermal conductivity and specific heat can change. More significantly, when decomposition occurs, fiber can be debonded from the resin and voids can be formed due to the decomposed gases. This can hamper the heat transfer within a composite material. However, the temperature range of the FRP bridge is between 20 to 60°C where the reduction of conductivity is less than 10% and increase of specific heat less than 10%.[26] Therefore, constant conductivity and specific heat is used in the thesis.

ISRR

iSRR is a new composite material of which there is no data could be found online, thus all the properties is calculated proportionally to its volume of contents (80%steel and 20%resin). iSRR has conductivity of $36.04 W/mK$, specific heat of $0.595 J/gK$, density of $0.00648 g/mm^3$, emissivity of 0.84.

3.1.2. PART

The Bridge deck is divided into different parts: FRP flange and web, connector, core, bolt center, bolt head and bolt nut. The FRP deck is assigned as GFRP material, connector assigned as iSRR material, core assigned as foam, all bolt parts assigned as steel.

FRP FLANGE AND WEB

FRP flange and web are made of vacuum infusion method together. According to the dimension in Figure2.2, the modeled part is shown below:

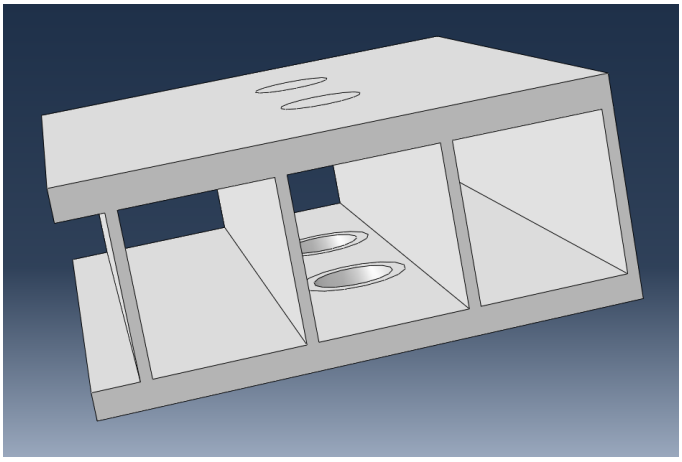

Figure 3.2: Part of FRP flange and web

CORE

The core full-fills the space within FRP deck except for the connector. According to the dimension in Figure2.2, the modeled part is shown below:

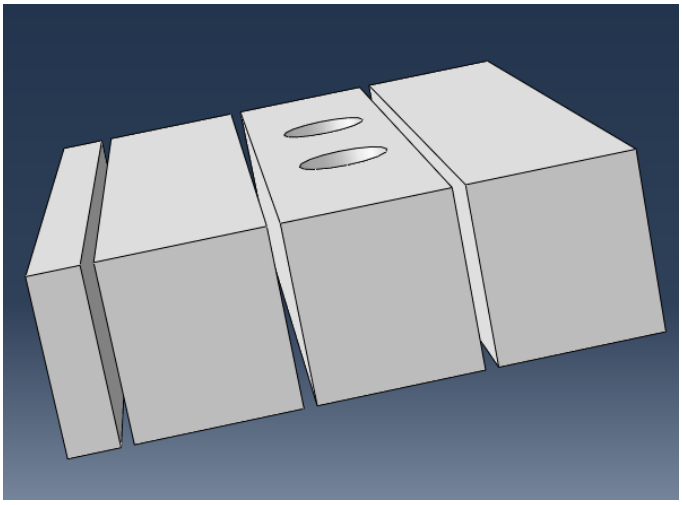

Figure 3.3: Part of Core

iSRR Connector

iSRR Connector could be divided into 2 parts: bolt and steel reinforced resin. Bolt is consisted of bolt center, bolt head and bolt nut, while the other space is full-filled with steel reinforced resin. According to the dimension of Figure2.3, the connector is shown below:

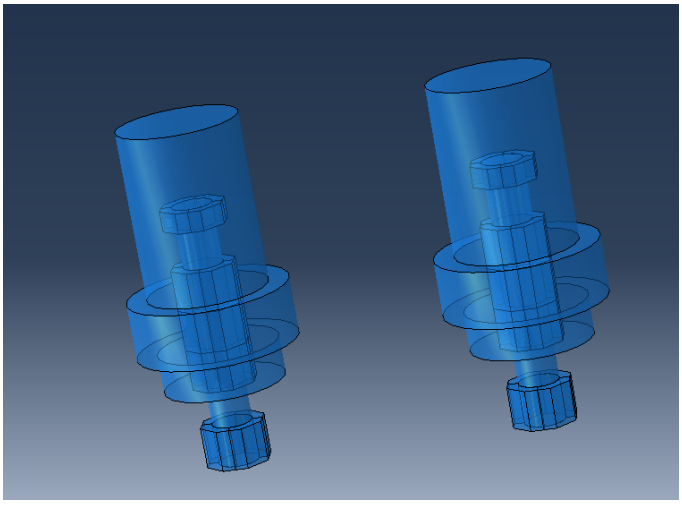

Figure 3.4: Part of iSRR connector

3.1.3. Assembly and interactions

Assembly

Put all the parts together, the final FRP deck is shown below:

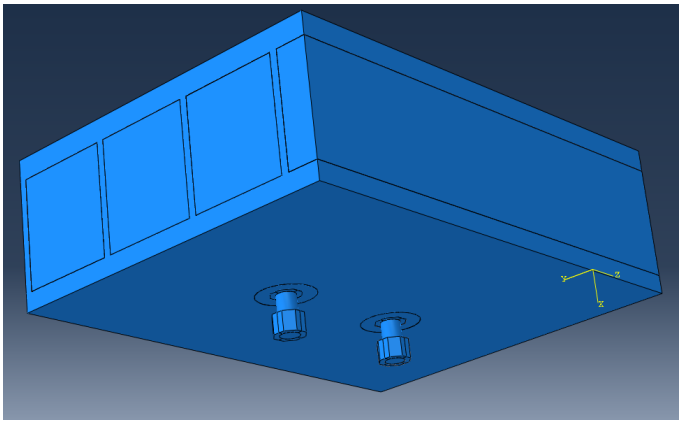

Figure 3.5: Assembly of FRP deck

INTERACTION

The interaction could be divided to 3 types: convection, radiation and conductance.

1. **Convection**
   For convection, in our case the FEM's vertical surfaces are all assumed covered with insulation panels, thus convection only happens at bottom surface and top surface of FRP flange. The convection of bottom surface is assumed to be half of that of the top surface according to Equation2.29 and Equation2.30. The convection of bottom bolt is neglected because of small surfaces.

   In Abaqus, the Surface film condition is used for representing convection, where the film coefficient represents convection coefficient and sink temperature represents ambient temperature. The convection coefficient will be calculated depending on experimental data, while the ambient temperature is the same as weather data in experiments.

2. **Radiation**
   For radiation, same as convection, only bolt and FRP flange at top and bottom surface has radiation emitted to the environment. In Abaqus, the surface radiantion is used to represent radiation, where emissivity and ambient temperature is needed according to table2.1 and weather data from experiments.

3. **Conductance**
   For conductance, it describes the time rate of steady state heat flow through a unit area of a material or construction induced by a unit temperature difference between the body surfaces[27]. In Abaqus, the surface-to-surface contact is used to represent conductance. It is assumed that all the surfaces are contacted tightly and heat can be thoroughly transferred between surfaces, thus a very big value is set for all the conductance.

3.1.4. STEP AND LOAD

INITIAL STEP

There are 2 steps in the FEM: initial step and heating step. In the initial step, the initial temperature of the specimen is set by predefined field. The value of the initial temperature depends on the experimental data.

HEATING STEP

Since the vertical surfaces are all covered by insulation panels, the heat resources in the heating step are the direct solar irradiance and the reflection from the ground.

1. **Solar irradiance**
   The direct solar irradiance is applied on the top surface of the deck with

homogeneous surface heat flux, and the magnitude of it is according to the weather data from KNMI.

2. **Ground reflection**
   The ground reflection is set as homogeneous heat flux on the bottom surface of the deck. Doigneaux found the albedo of grass is about 0.18 to 0.23 in 1973[28]. What's more, Monteith found a variation in the reflectance of short grass of about 0.22 at a solar altitude of 60° to 0.28 at a solar altitude of 20°.Since the ground material of experimental environment is grass and the latitude of experimental location is 52°, the Ground albedo is set about 0.23. Therefore, the magnitude of the ground reflection is about 0.23 times solar irradiance.

3. **Step time**
   The simulation of the FEM are divided into 2 types according to time duration: 15min (20min for 9-02) and 7h. Changing amplitude is applied according to the time of the day for the heat flux.

3.1.5. MESH

MESH ALGORITHM

There are two algorithms in Abaqus when it comes to mesh: Medial axis and Advancing front.
The medial axis algorithm first decomposes the region to be meshed into a group of simpler regions. The algorithm then uses structured meshing techniques to fill each simple region with elements. If the region being meshed is relatively simple and contains a large number of elements, the medial axis algorithm generates a mesh faster than the advancing front algorithm[29].
The advancing front algorithm generates quadrilateral elements at the boundary of the region and continues to generate quadrilateral elements as it moves systematically to the interior of the region[29].
Abaqus will choose the algorihms by default after you choosing the element type and technique at most time.

ELEMENT SHAPE

Hex is a hexahedron element, it has a very good accuracy and reduces solver time.

Tet is a tetrahdral element, it is easy to mesh with Tet because most geometry can be divided into tetrahedral shapes. However results could be poor for tets with bad aspect ratio and linear elements.

Table 3.1: Mesh size and type for different parts

Part	Mesh size (mm)	Element shape	Technique
Bolt center	2.8	Hex	Sweep
Bolt head	1.4	Hex	Structured
Bolt nut	2.0	Hex	Structured
Core(with holes)	20	Tet	Free
Core (solid)	20	Hex	Structured
FRP flange and web	20	Tet	Free
iSRR	10	Tet	Free

3.2. EXPERIMENT

The experiment is designed to validate the FEM. Get the temperature change of the FRP deck specimens under sun light in natural environment considering solar irradiance, ambient temperature and wind speed. And validate Abaqus model with the result.

3.2.1. PLAN OF THE EXPERIMENT

EXPERIMENT EQUIPMENT

The infrared camera from Flir is used to record the surface temperature of the specimen. The thermal image of the infrared camera can record the temperature of each pixel and time information. The temperature of the pixel will be transferred into specimen's real length scale in result progressing part.
Although it will be perfect if we can detect the inside temperature within connector, there is neither equipment available to detect inside temperature, nor possibility to apply sensors into the specimen after the manufacture of the deck.

EXPERIMENT PREPARATION

1. Find two FRP deck specimen with the same dimension as the FEM in Abaqus.

2. Use the insulation panels to cover the vertical surfaces around the specimens, therefore, the top and bottom surfaces are the only heated surfaces just the same as FEM.

3. Paint the top surface of one specimen into black and keep the other one of the original color. Since the FEM is considered as black body, all radiation is assumed to be absorbed by the surfaces. Black color has the most similar properties with black body. Besides, it is a brief comparison to see the color influence to the solar irradiance absorption. The prepared specimens are shown in the Figure3.6.

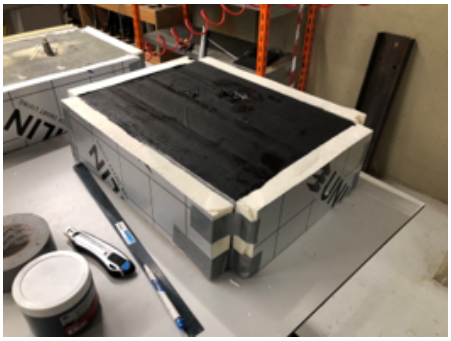
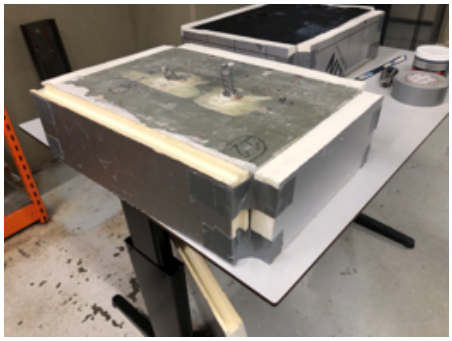

Figure 3.6: Left: black specimen, Right: original color specimen

EXPERIMENT PROCEDURE

1. Choose a warm day and put the specimen on the lawn horizontally under the sun light. The specimen should be put above the ground for about 0.5m high to ensure it will not conduct heat with the ground. The experiment site is shown in Figure3.7.

Figure 3.7: Experiment site

2. Take the surface temperature (foam side, web side and top) every 5min during 1 h at around 14:00. The side picture is taken when the covered panel is temporarily lifted manually. Because the lifted time is very short compared to the whole experiment duration, the heat up of the side surface is neglected. The picture taking process is shown in Figure3.8.

3. Take the surface temperature (foam side, web side and top) every 30min during the whole warm day to see how temperature accumulates within the specimen.

Figure 3.8: Taking thermal images

LIST OF EXPERIMENTS

To get the as high temperature as possible, The experiment date is mainly chosen in September and experiment time should include the hottest duration in the day, at around 14:00. Although a lot of experiments are done, some of them can't be used because of manual operation deviation.Here is the list of the experiments:

Table 3.2: List of experiments

Experiment	Date	Time	average ambient T (°C)	average wind speed (m/s)	highest Irradiance (W/m2)
6-22-60min	22-6-2022	14:40-15:45	24.2	3.67	905
9-02-45min	02-9-2022	14:00-14:45	25.1	5.51	712.0
9-02-30min	02-9-2022	16:30-17:00	25.9	5.88	535.0
9-03-55min-1	03-9-2022	11:45-12:40	23.4	3.46	660.0
9-03-55min-2	03-9-2022	14:55-15:50	26.6	3.41	667.5
9-05-60min	05-9-2022	14:15-15:15	29.9	4.35	695.5
9-06-85min	06-9-2022	12:45-14:10	23.6	4.45	677.0
9-07-7h	07-9-2022	10:20-17:10	22.0	5.56	698.5
9-08-65min	08-9-2022	14:25-15:30	21.1	6.12	645.0
9-12-7h	12-9-2022	10:40-17:30	22.2	4.26	655.0

DATA PROCESSING

There are mainly 4 kinds of infrared thermal image: top surface, side surface of web, side surface of core and side surface of core & web. The images will be edited in FLIR tool software.

1. **Top surface**
   The Top surface has the highest temperature of the specimen, but the temperature on the surface is not even due to the defect of manufacturing. Therefore, the average temperature is calculated with the FLIR tool. Choose a box tool to include the top surface, the average, minimum, maximum temperature will be calculated within the box.

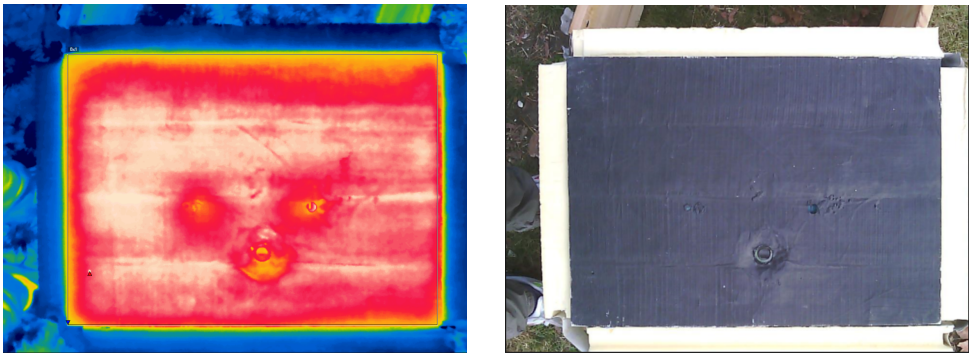

Figure 3.9: Left: Thermal image of the top surface, Right: Original image of top surface

2. **Side surface of web & core**
   The thermal image of the side surface of web & core shows the temperature gradient on the short side surface of the deck. Three lines are chosen separately along the web of the side surface. The extracted temperature along the line is scaled into the real height of the specimen which is $153.5mm$.

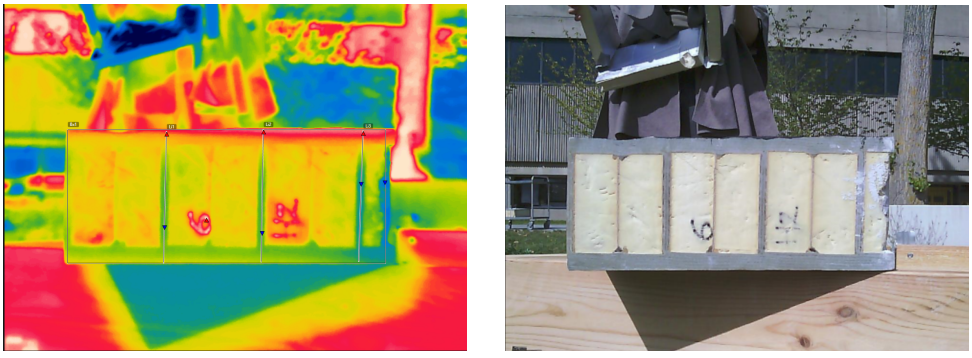

Figure 3.10: Left: Thermal image of the side surface of web & core, Right: Original image of the side surface of web & core

3. **Side surface of web**
   The thermal image of the side surface of web shows the temperature gradient along the web in the long side surface.Three lines are chosen separately on the side surface of web. The extracted temperature along the line is scaled into the real height of the specimen which is 153.5mm. The image in the Figure3.11 is in the color of foam because the web surface has some remaining foam after being cut into specimen size which could be neglected.

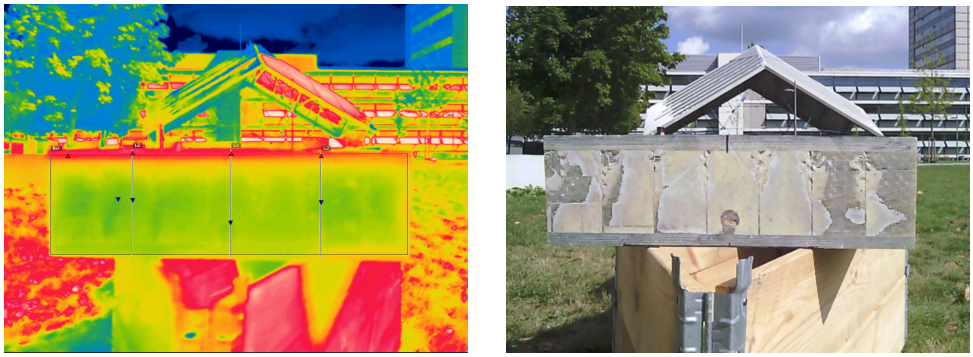

Figure 3.11: Left: Thermal image of the side surface of web, Right: Original image of the side surface of web

4. **Side surface of core**
   The thermal image of the side surface of core shows the temperature gradient along the core material along the thickness of the deck. Three lines are chosen separately along the side surface. The extracted temperature along the line is scaled into the real height of the specimen which is 153.5mm.

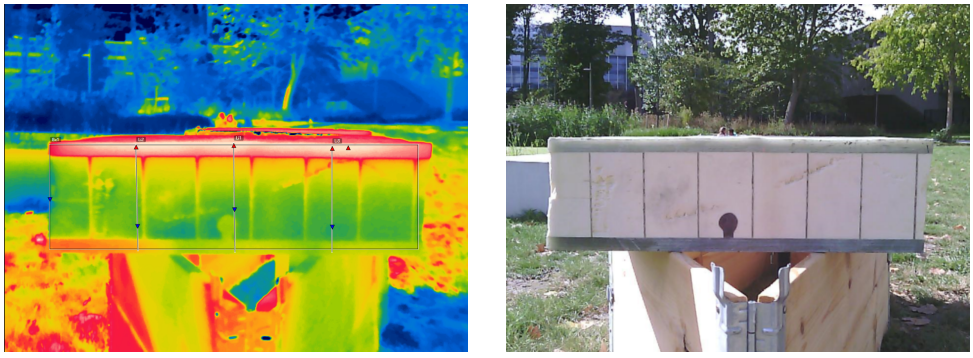

Figure 3.12: Left: Thermal image of the side surface of core, Right: Original image of the side surface of core

The example of extracted temperature along the side surface is shown in Figure3.13. The detailed table of side temperature is in Appendix B.

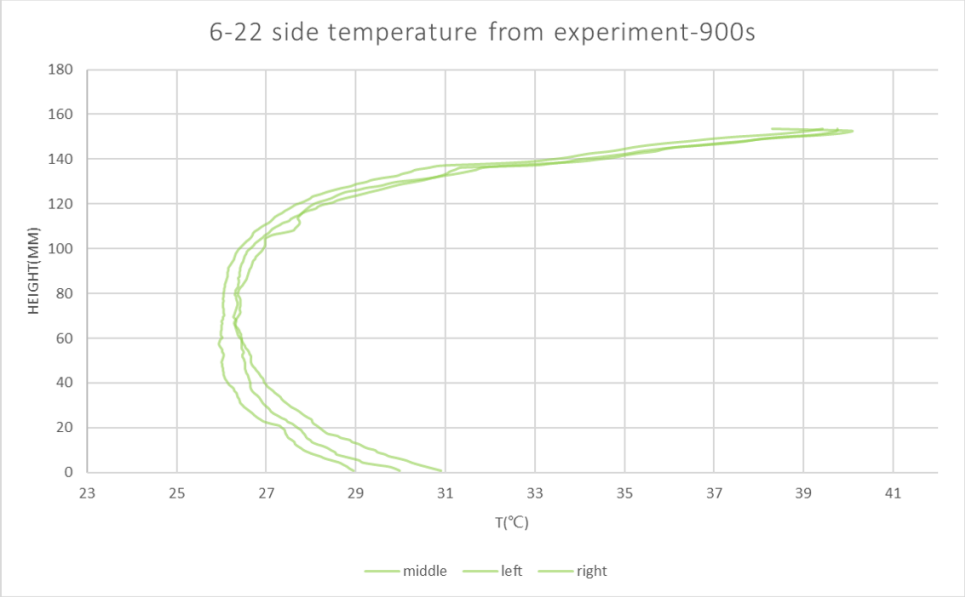

Figure 3.13: Side temperature of 22-6-2022

4

RESULT

4.1. RESULT OF EXPERIMENT

The results from the experiment are sorted into average temperature of top surface, side temperature of web, side temperature of core. Although two specimens are used in the experiment, the side temperature of the original color specimen is not studied because of the dimension difference with the FEM. Only in the average temperature of the top surface part the original color specimen is considered to see the influence of color on the solar irradiance absorption.

4.1.1. AVERAGE TEMPERATURE OF TOP SURFACE

It is obviously the top surface will have the highest temperature when the bridge deck is heated up by sun light in natural environment. This temperature is very important because the strength of the FRP suffers from reduction when temperature rises. And the top flange of the FRP is just the part bears most compression stresses. The rate of temperature change and highest temperature are the main subjects we are concerned. The short time period result and long time period results are all shown in Figure4.1 and Figure4.2:

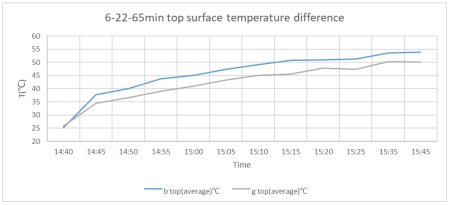

(a) 6-22

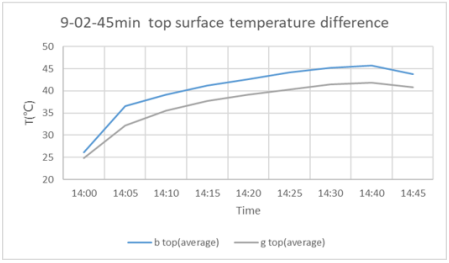

(b) 9-02-1

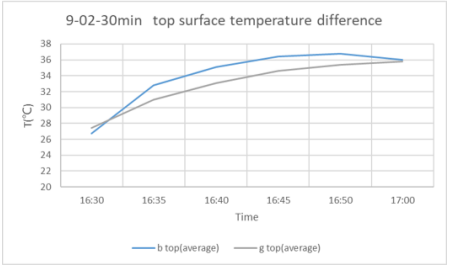

(c) 9-02-2

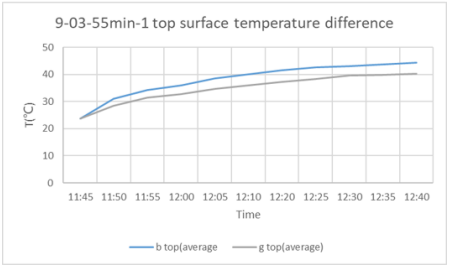

(d) 9-03-1

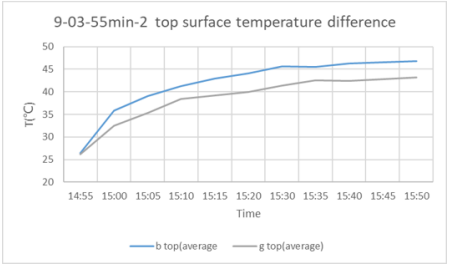

(e) 9-03-2

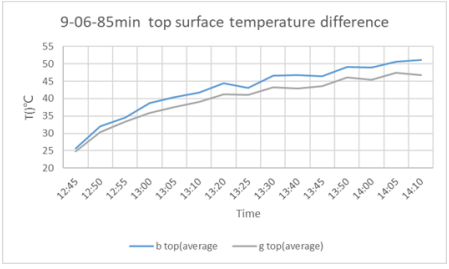

(f) 9-06

Figure 4.1: Average top temperature of short time period experiments

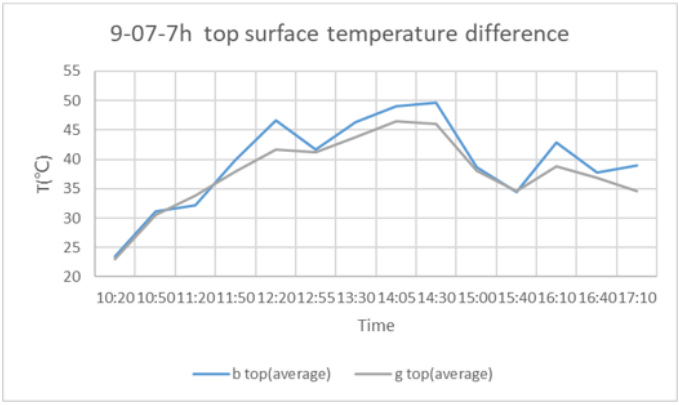

(a) 9-07

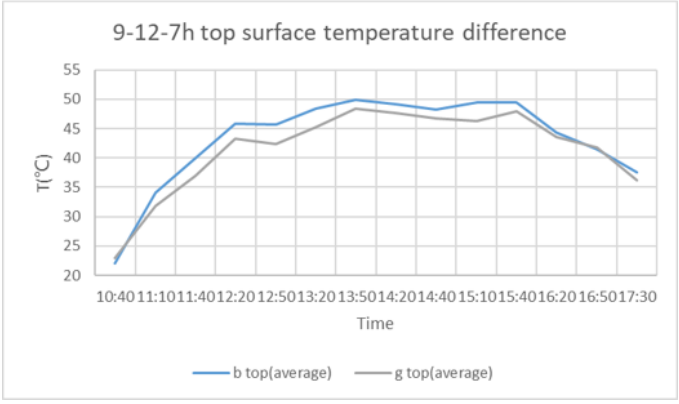

(b) 9-12

Figure 4.2: Average top temperature of long time period experiments

ANALYSIS

The blue line is the average top temperature of black specimen while the grey line is of original color (dark green). The maximum temperature among all the experiments is 53.9°C on 15:45, 22-6-2022. This temperature could lead to tensile strength reduction up to 60%[2].
According to the table4.1, maximum rate of temperature rising on the top surface is 0.80°C/min, which means the temperature could rise rapidly for 24°C when it is exposed to sun light in summer. Since the dark color usually has lower albedo and high emissivity, the black specimen is heated up faster and cooled down faster too. In table4.1, the difference of temperature rising rate between black specimen and green specimen increases with solar irradiance, of which the maximum is 0.16°C/min. But from the Figure4.1and Figure4.2, the maximum accumulated temperature difference will be no more than 5.2°C. As the experiment time is mainly at daytime, the top surface temperature of the black specimen is always higher than that of original color specimen.

Table 4.1: Rate of temperature rising for the first 30mins

Experiment	Time	speed of black(°C/min)	speed of green(°C/min)
6-22-60min	14:40-15:45	0.80	0.64
9-02-45min	14:00-14:45	0.64	0.56
9-02-30min	16:30-17:00	0.31	0.28
9-03-55min-1	11:45-12:40	0.59	0.46
9-03-55min-2	14:55-15:50	0.64	0.51
9-06-85min	12:45-14:10	0.62	0.55

Looking at the temperature accumulation during day time of 07-9-2022 and 12-9-2022, the maximum temperature of the date 9-07 is reached at 14:30 and the maximum temperature of the date 9-12 is reached at 13:50. Compare the curve of temperature to the curve of irradiance during the day from Figure4.3, a high similarity could be found: the maximum irradiance is reached at 14:05 for date 9-07 while the maximum irradiance is reached at 14:20. And the temperature of the top surface decreases immediately when the irradiance decreases according to the curve after 14:00. A brief conclusion could be made that the irradiance is the most important factor that influence the temperature of the top surface because the heat up process and emission process are both very fast for FRP bridge deck.

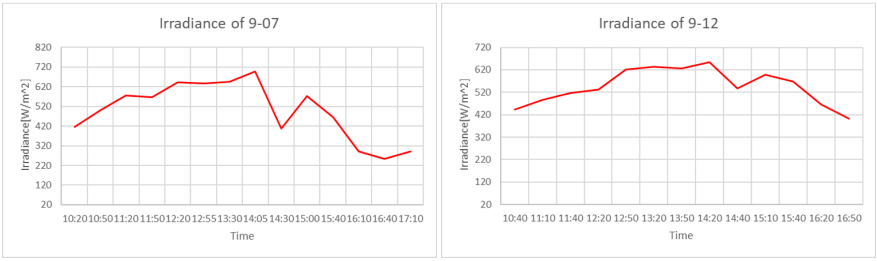

(a) Irradiance of 9-07 (b) Irradiance of 9-12

Figure 4.3: Irradiance of whole day experiments

4

4.1.2. SIDE TEMPERATURE OF FOAM AND FRP WEB

Foam is a well-known insulation material which has low conductivity, as expected the temperature of foam should change slower than that of FRP webs. The temperature of the side surface of web & core as Figure3.10 mentioned is shown below:

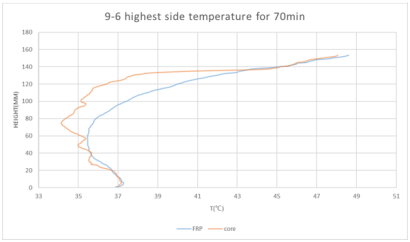

(a) Short time period 9-06

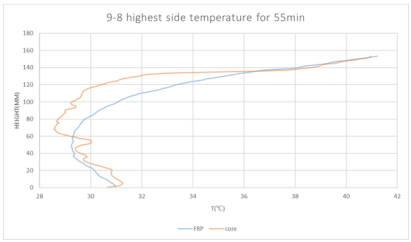

(b) Short time period 9-08

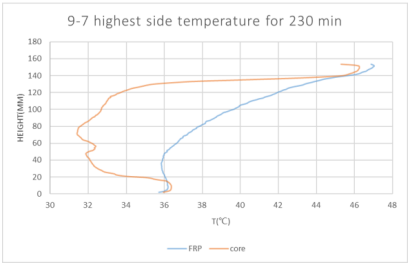

(c) Long time period 9-07

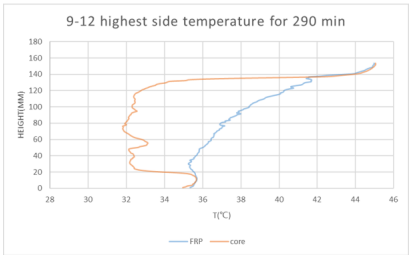

(d) Long time period 9-12

Figure 4.4: Side temperature difference between core and FRP

ANALYSIS

As the Figure4.4 shows, when heat up time is short, the temperature difference between core and FRP grows with the distance with the top and bottom surface. And the average maximum temperature difference is about 3.79°C at the height of 131mm as shown in Figure4.5.
As for long time period experiments, the average maximum temperature difference is about 7.96°C at the height of 121mm as shown in Figure4.5 too.
Combining the short time period result and long time result, the temperature difference between core and FRP web grows with the distance with top and bottom surface and also grows with time of heating. This temperature difference may not be neglected if the delamination between core and FRP will happen. However, the FRP temperature is more important and this question is left for further researches.

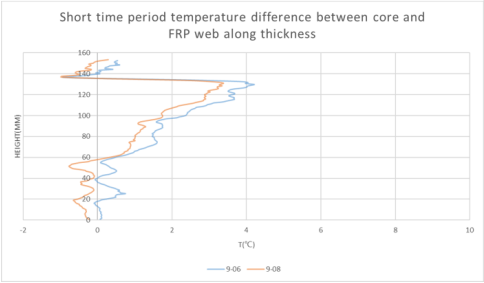

(a) Short time period temperature difference between core and FRP web

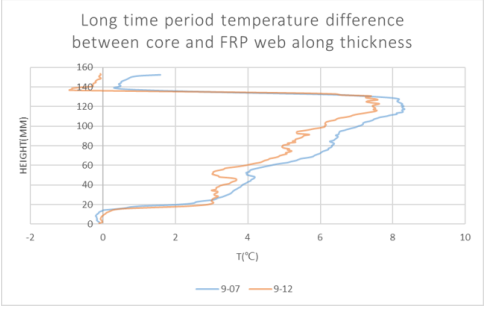

(b) Long time period temperature difference between core and FRP web

Figure 4.5: Temperature difference between core and FRP web along thickness

4.2. VALIDATION OF THE FEM

Since the temperature of the FRP influence the mechanical properties of the whole FRP deck, the side temperature of the FRP web of the black specimen is chosen for the validation of the FEM result.

4.2.1. OPTIMIZATION OF FEM RESULT

As mentioned in the Chapter2, the material properties are set according to the data in other researches, which may not match the real material used in the experiment. It is necessary to make adjustment on the material properties to optimize the FEM simulation result.

The adjustment is based on the simulation result of experiment 6-22. The conductivity, specific heat, density of foam and FRP are changed to see the influence on the simulation.

FOAM PROPERTIES

1. **Specific heat**
   The specific heat is reduced by 50% from $1.47 J/Kg$ to $0.735 J/Kg$. And the result shows that the influence to FRP web is very tiny according to Figure4.6.

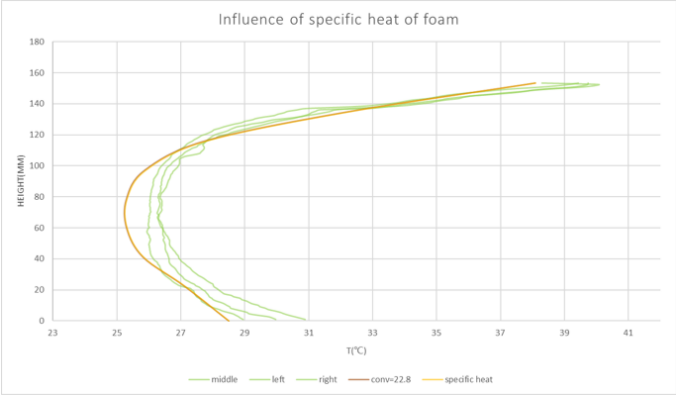

Figure 4.6: Influence of foam's specific heat

2. **Density**
   The density is reduced by 50% from $6 \times 10^{-5} g/mm^3$ to $3 \times 10^{-5} g/mm^3$. And the result shows that the influence to FRP web is also very tiny according to Figure4.7.

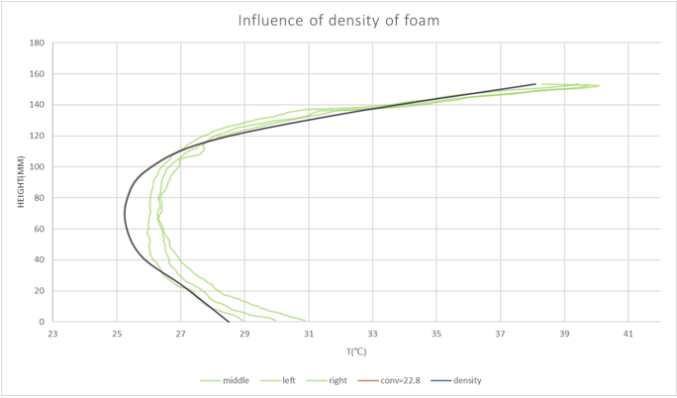

Figure 4.7: Influence of foam's density

3. **Conductivity**
   The conductivity is reduced by 50% from $0.02 W/mK$ to $0.01 W/mK$. And the result shows that the influence to FRP web is very tiny as well according to Figure4.8.

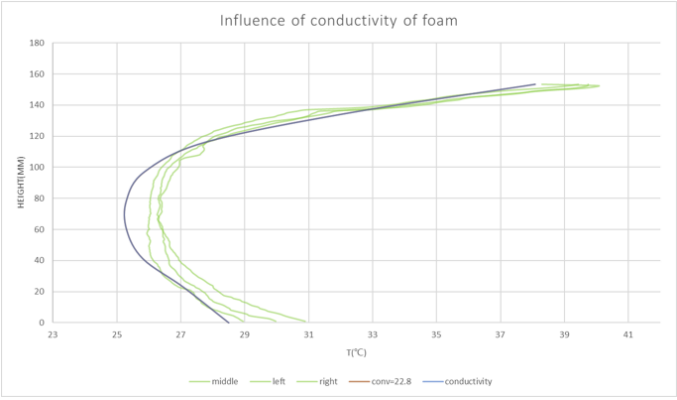

Figure 4.8: Influence of foam's conductivity

FRP PROPERTIES

1. **Specific heat**
   The specific heat is reduced by 20% from $1.287 J/Kg$ to $1.03 J/Kg$. And the result shows that the temperature of whole FRP web increased but the slope of the plot stays the same. The result is shown in Figure4.9.

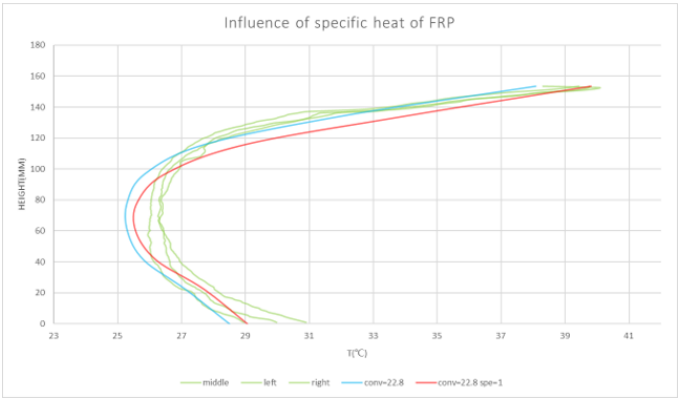

Figure 4.9: Influence of FRP's specific heat

2. **Density**
   The density is reduced by 20% from $1.6 \times 10^{-3} g/mm^3$ to $1.28 \times 10^{-3} g/mm^3$. According to Figure4.10, the temperature of whole FRP web increased but the slope of the plot stays the same.

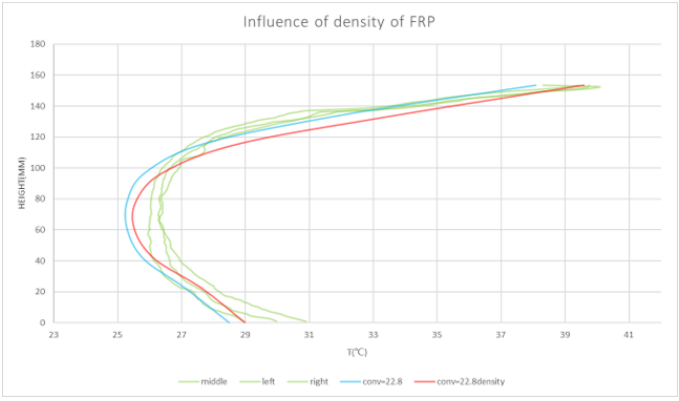

Figure 4.10: Influence of FRP's density

3. **Conductivity**
   The conductivity is increased by 20% from $1.36 W/mK$ to $1.632 W/mK$. According to Figure4.11, the temperature of top surface and bottom surface decreases a little bit while the temperature of the middle part increases a little bit.

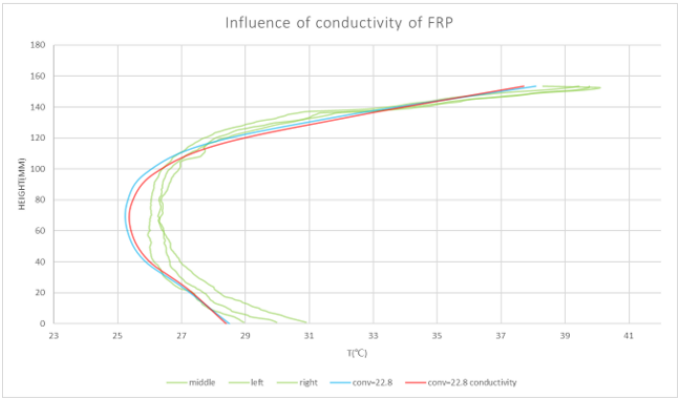

Figure 4.11: Influence of FRP's conductivity

ANALYSIS

Heat diffusivity is the thermal conductivity divided by density and specific heat capacity at constant pressure, and it represent the rate of temperature change.[30]

1. The foam properties nearly have no influence on the temperature of FRP web. The reason is that the product of specific heat capacity and density of foam ($8.82 \times 10^{-5} J/(K \cdot mm^3)$) is relatively low compared to that of FRP ($2.06 \times 10^{-3} J/(K \cdot mm^3)$), which means the heat energy is mostly absorbed by FRP.

2. Decreasing the density and specific heat of FRP have the same influence of the temperature of FRP web: change the temperature of the whole FRP web surface in a similar extent. The plot will move parallel in horizontal direction in the figure. This reason is that less energy is needed for the temoperature rising.

3. When Increasing the conductivity of FRP web not only increase the temperature of middle part of the FRP web surface, but also decrease the temperature of top and bottom surface. The plot will have sharper slope in the figure. This reason is that the heat energy will be transferred faster into inside of the specimen.

OPTIMIZATION

Combining all the change above, finally the conductivity of FRP is changed from $1.36 W/mK$ to $0.85 W/mK$. In this case, the FEM results are improved in predicting experimental results.

4.2.2. VALIDATION OF THE CONVECTION MODEL

As mentioned in the Chapter2, the variables of natural convection and mixed convection should be decided by test results. But the variables used in this thesis are from other tests which have different material and experimental environment with our case. The convection model should be validated.

1. **Surface of convection**
   Convection influences the top surface and bottom surface. Assume that the material properties are correct, then the change of convection coefficient will influence the temperature of top surface and bottom surface. Meanwhile, the assumption made in Chapter 3 is that the convection coefficient of the bottom surface is half of that of the top surface. As a result, by changing the convection coefficient of the top surface and compare the temperature of the top part of FRP web surface (Figure3.11) can validate the convection model.

2. **Variable to be compared**
   Since the top surface temperature is sensitive to environmental influences that may not be considered in FEM, the slope of thickness to temperature of the top $19mm$ is compared between FEM results and experimental results. The best matched convection coefficient will be compared with theoretical value.

3. **Time period**
   The weather should not change too much in the time period and the temperature should be obvious enough for comparison. Therefore, the first 15 min of short time period experiments and first 30min of long time period experiments (9-07 and 9-12) are chosen to be input of FEM simulation.

THE BEST FIT CONVECTION COEFFICIENT

The results of the best fit convection coefficient is shown in Table4.2. The convection coefficient of FEM and theoretical calculation have a large difference at first sight. Further processing should be done to see the clear comparison.

Table 4.2: Best matched convection coefficient and slope

Date	convection coefficient (W/(m2 K)	Slope of FEM	Slope of experiemnt
6-22	22.8	2.28	2.27
9-02	12	2.47	2.48
9-03	15	2.91	2.89
9-05	40	3.19	3.45
9-06	20	3.13	3.07
9-07	26.9	6.56	6.5
9-12	13.7	4.16	4.09

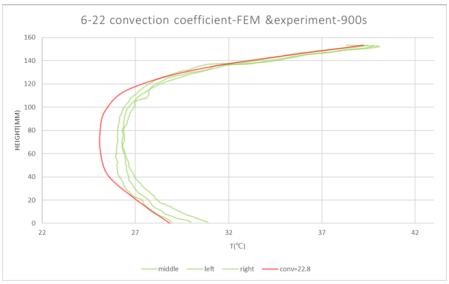

(a) 6-22

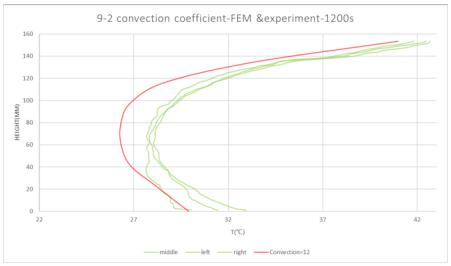

(b) 9-02

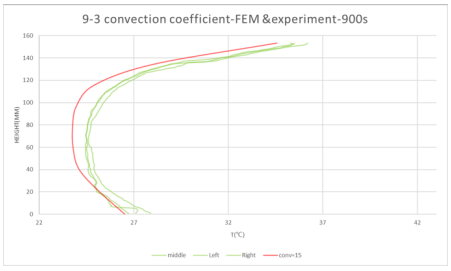

(c) 9-03

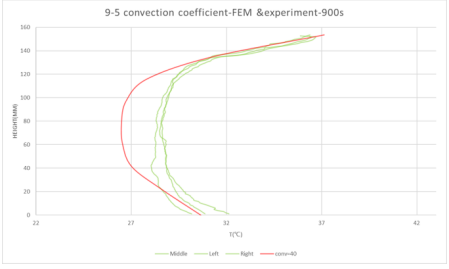

(d) 9-05

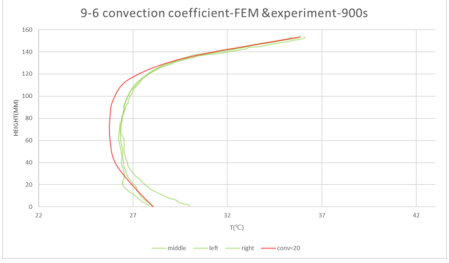

(e) 9-06

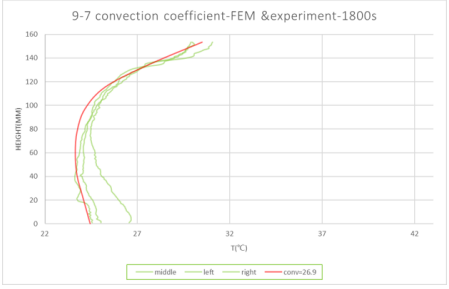

(f) 9-07

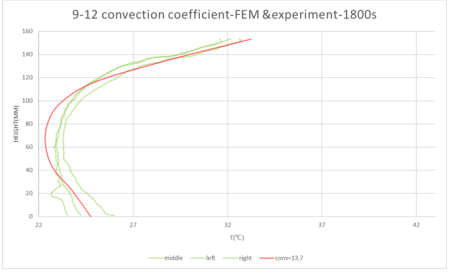

(g) 9-12

Figure 4.12: Best matched convection coefficient according to experimental results

FUNCTION OF CONVECTION COEFFICIENT

Since the convection coefficient is calculated with top surface temperature difference with air and wind speed, we try to find the relationship between convection coefficient and wind speed, top surface temperature difference. Finding easy function to calculate convection coefficient with simple weather data like ambient temperature will help a lot in the real engineering design.

Table 4.3: Convection coefficient and related wind speed, ΔT

Date	ΔT(°C)	Ambient T(°C)	Wind speed(m/s)	From FEM convection coefficient ($W/(m^2K)$)	From calculation convection coefficient ($W/(m^2K)$)
6-22	19.59	24.11	3.71	22.8	22.8
9-02	17.73	24.87	5.25	12.0	27.1
9-03	13.05	23.05	3.90	15.0	23.4
9-05	10.61	29.99	4.58	40.0	25.3
9-06	15.37	23.33	5.02	20.0	26.5
9-07	11.10	19.73	3.97	26.9	23.6
9-12	13.95	20.15	4.53	13.7	25.2

1. **Temperature difference between top surface and air**
   The ΔT is calculated at the end of the test time period. As the Table4.4 shows, the influence of ΔT is very limited when deciding the value of convection coefficient using theoretical calculation when ΔT is the range of experimental results.
   Besides, the temperature difference is not practical in real engineering design.

Table 4.4: Convection coefficient change with wind speed and ΔT

Convection coefficient ($W/(m^2K)$)	$\Delta T1$(°C)	$\Delta T2$(°C)
wind speed(m/s)	5.00	30.00
1.00	11.90	12.16
2.00	16.76	16.87
3.00	20.51	20.58
4.00	23.66	23.72
5.00	26.46	26.50
6.00	28.98	29.00
7.00	31.30	31.33
8.00	33.46	33.46
9.00	35.49	35.49
10.00	37.41	37.41

2. **Wind speed**
   The wind speed shows good relationship with convection coefficient in theoretical calculation according to Table4.4. If the convection model is validated by the Experimental results, it will be an excellent variable to calculate convection coefficient in a simple function.
   According to the Figure4.13, the experimental results locate evenly around the theoretical results which is acceptable in statistic analysis. And the variance

becomes larger as wind speed increases. Therefore, the theoretical result is validated.

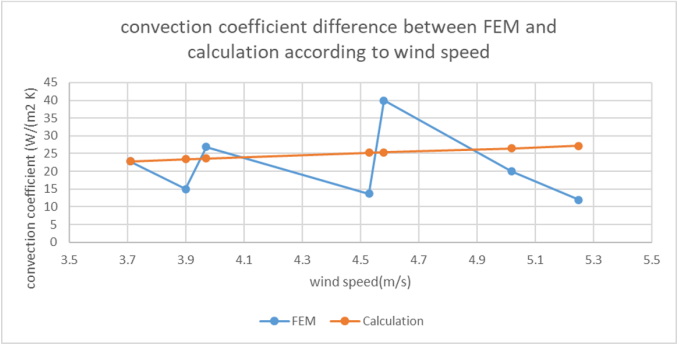

Figure 4.13: Convection coefficient to wind speed

The expected function of convection coefficient to wind speed is got by the interpolation (Figure4.14) of theoretical results:

$$y = 2.7992V + 12.471 \tag{4.1}$$

Where V is wind speed.

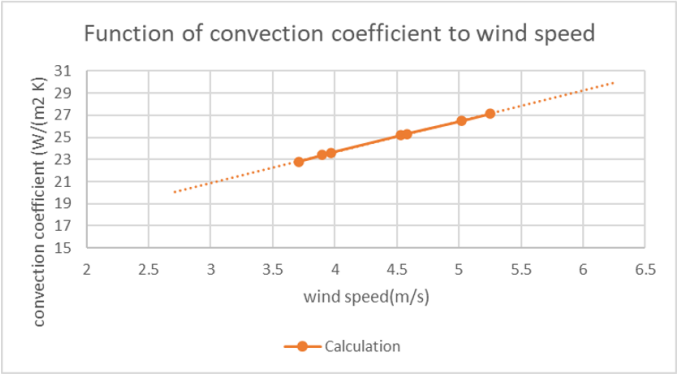

Figure 4.14: Function of convection coefficient to wind speed

4.2.3. VALIDATION OF THE WEB-CORE DIFFERENCE

The temperature difference between web and core comes from 2 parts.

DIFFERENCE FROM MATERIAL PROPERTIES

First, the difference of the thermal properties of FRP and foam has influence. Conductivity is a measure of its ability to conduct heat, specific heat is the heat capacity

of a sample of the substance divided by the mass of the sample. To compare the rate of temperature change between two materials, thermal diffusivity combines thermal conductivity with density and specific heat:

$$\alpha = \frac{k}{\rho c_p} \tag{4.2}$$

α: thermal diffusivity
k: thermal conductivity
ρ: density
c_p: specific heat

Calculated with the data from Table 2.1, thermal diffusivity of FRP is $0.66 W \cdot mm^2/J$ and thermal diffusivity of foam is $0.227 W \cdot mm^2/J$.In a brief conclusion is that the temperature of FRP material changes 3 times faster than that of foam.

INFLUENCE OF CONDUCTANCE

When two solid bodies come in contact, such as A and B in Figure 1, heat flows from the hotter body to the colder body. From experience, the temperature profile along the two bodies varies, approximately, as shown in the figure. A temperature drop is observed at the interface between the two surfaces in contact. This phenomenon is said to be a result of a thermal contact resistance existing between the contacting surfaces. Thermal contact resistance is defined as the ratio between this temperature drop and the average heat flow across the interface.[31] And the thermal conductance is the inverse of the thermal resistance.

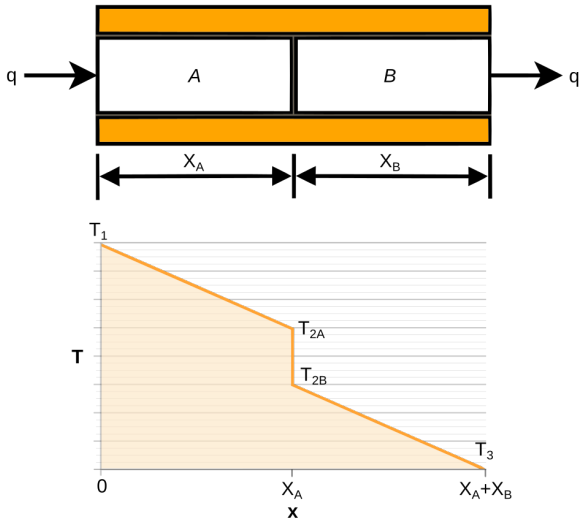

Figure 4.15: Introduction of conductance

From the manual of Abaqus, the flow between the two surfaces in contact is assumed to be defined by

$$q = k(\theta_A - \theta_B),$$

where q is the heat flux per unit area crossing the interface from point A on one surface to point B on the other, θ_A and θ_B are the temperatures of the points on the surfaces, and k is the gap conductance.

As there is no reference available for the indicative value of conductance between FRP material and foam, the conductance value here is tested by comparing simulation result to experimental result of date 9-06. From the equation above, an obvious relationship between temperature gap and conductance is found: the smaller conductance, the bigger temperature gap if the energy is constant. By decreasing conductance from $1 \times 10^{-4} W/(mm \cdot K)$ to $1 \times 10^{-7} W/(mm \cdot K)$, the relationship between conductance and web-core temperature difference is found.

From the shape of the temperature curve of the core in the figures, it could also be seen that the slope from height of 40mm to 120mm are much higher than before which means the temperature gradient within the foam material is much smaller. From height of 134.5mm to 153.5mm, the temperature of FRP above the core is a little bit higher than that of FRP above FRP web. This phenomena is also as expected because heat transfer between flange and core is slower between flange and web. Therefore, the heat energy above the core is slightly higher than that of obove the web.

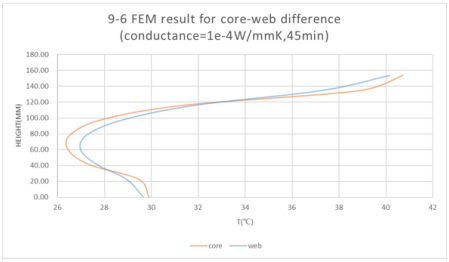

(a) conductance=1×10^{-4}

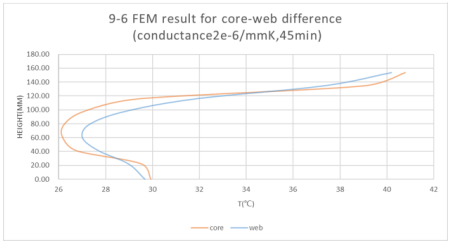

(b) conductance=2×10^{-6}

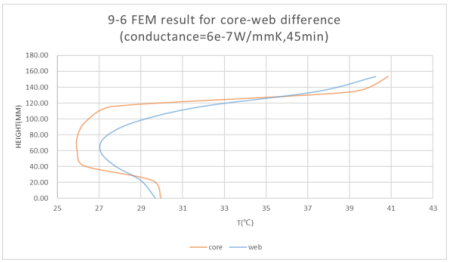

(c) conductance=6×10^{-7}

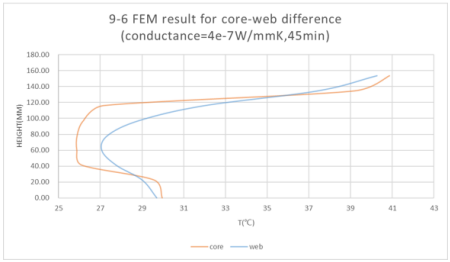

(d) conductance=4×10^{-7}

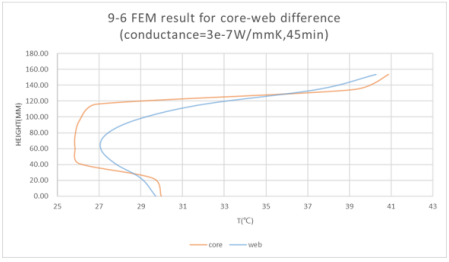

(e) conductance=3×10^{-7}

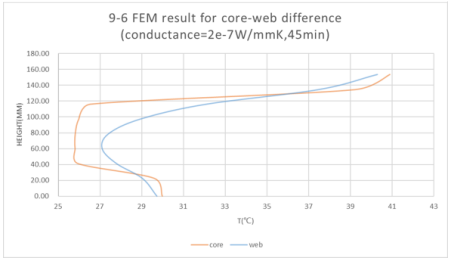

(f) conductance=2×10^{-7}

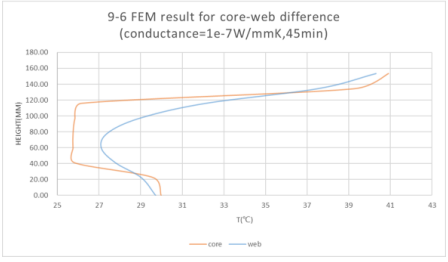

(g) conductance=1×10^{-7}

Figure 4.16: Temperature difference between web and core with different conductance in FEM

To quantify the sensitivity of the conductance change to the temperature difference between web and core, the summed absolute value of temperature difference along the thickness of the deck is calculated. Divide the thickness of the deck into 9 parts evenly and add up the absolute value of the temperature difference of core and web at these heights. The result is shown in Table4.5 and Figure4.17.

The temperature difference between web and core increases slowly when conductance between web and core decreases. However, when the conductance is smaller than $2 \times 10^{-6} W/(mm \cdot K)$, the temperature difference immediately has a sharp increase with the decrease of conductance.

The reason for this phenomena should be that the speed of heat transferred between core and FRP is mostly within the range of $2 \times 10^{-6} W/(mm \cdot K)$. As the conductance set between the core and web is the maximum speed limit for the heat energy transferred across the contacted surfaces and the speed of heat transfer is less than$2 \times 10^{-6} W/(mm \cdot K)$ for the most time, the high conductance value have limited influence on the temperature difference between web and core.

Table 4.5: Absolute value of temperature difference of web and core

Conductance$W/(mm \cdot K)$	Absolute temperature difference(°C)
1×10^{-4}	5.97
2×10^{-6}	10.09
6×10^{-7}	13.88
4×10^{-7}	14.98
3×10^{-7}	15.64
2×10^{-7}	16.38
1×10^{-7}	17.24

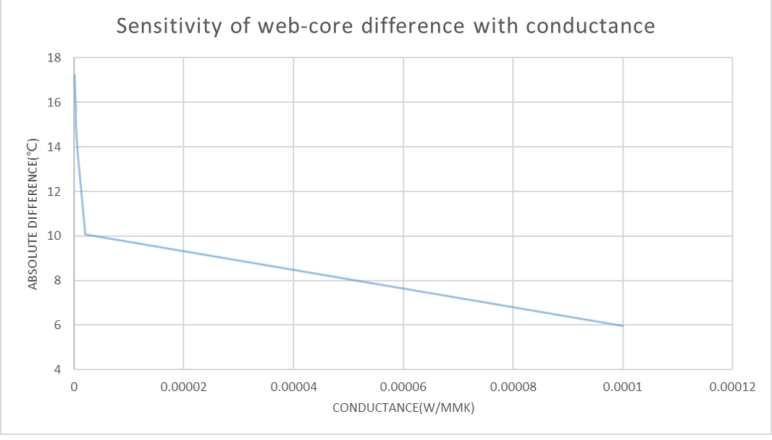

Figure 4.17: Sensitivity of conductance to the temperature difference between web core

VALIDATION OF WEB-CORE DIFFERENCE

The highest top surface temperature of experiment on date of 07-09-2022 is reached at 14:30, and this experimental data is used to validate the web-core temperature difference of FEM simulation. Different values of conductance are tested in the simulation. In the end, the simulation result fits the experiment result best when conductance is $2\times10^{-7}W/(mm\cdot K)$. To quantify the validation,as the Table4.6 shows, the slope of the core temperature between height of 40mm and 120mm is compared and the slope of FEM is 0.035, slope of experiment is 0.021. The absolute temperature difference is compared, absolute ΔT is 30.14°C for FEM, absolute ΔT is 38°C for experiment. And the maximum temperature difference is also compared, the maximum ΔT is 7.98°C for FEM, the maximum ΔT is 8.27°C for experiment. The Figure4.18 shows the result of temperature curves from both FEM simulation.

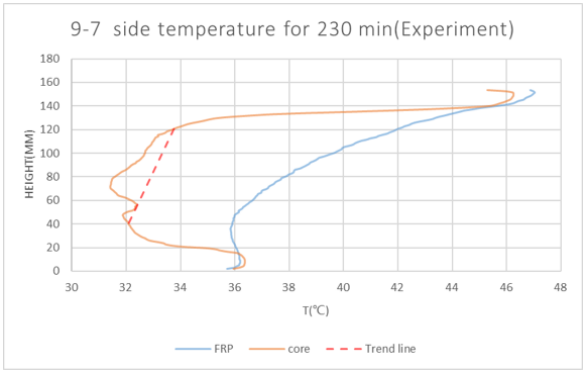

(a) Experiment

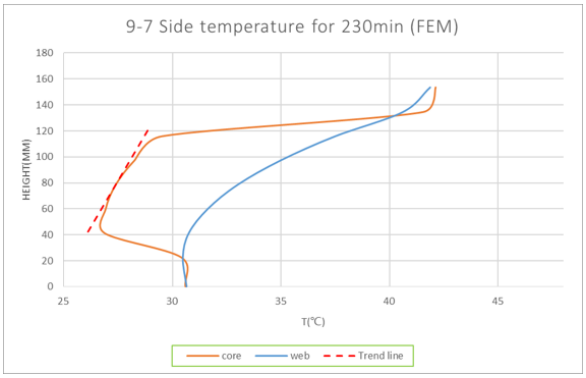

(b) FEM simulation

Figure 4.18: Comparison of simulation result and experiment for web-core temperature difference

Table 4.6: Comparison of simulation and experiment for web-core temperature difference

	FEM	Experiment
Absolute Δ T (°C)	30.14	38.00
Slope of core temperature	0.035	0.021
Maximum Δ T (°C)	7.98	8.27

4.2.4. VALIDATION OF DAY TIME SIMULATION

As shown in the Figure4.12, the FEM have a relatively good prediction for the short time period experiment. Then the FEM should also be tested for a long time period prediction. Take the experimental data of 9-07 as test target, several simulations are made.

RESULT FROM FEM AND EXPERIMENT

Since the side surface temperature of web could best represent the temperature condition of the specimen, the change of side surface temperature is recorded with time. The radiance and ambient temperature are got from the weather data of KNMI. And the convection coefficient is calculated with the simplified function got in Equation4.1.

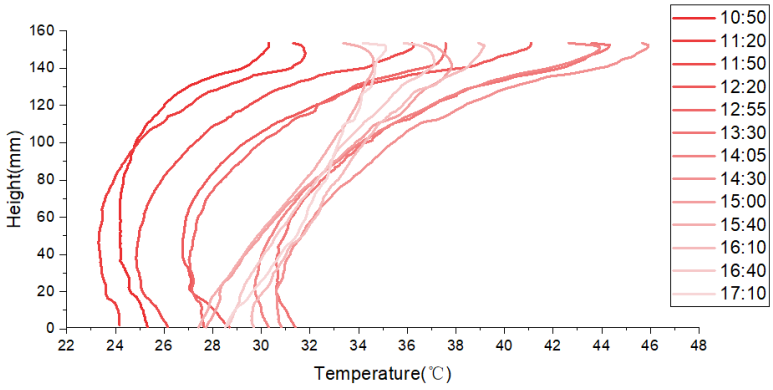

(a) 9-07Experiment

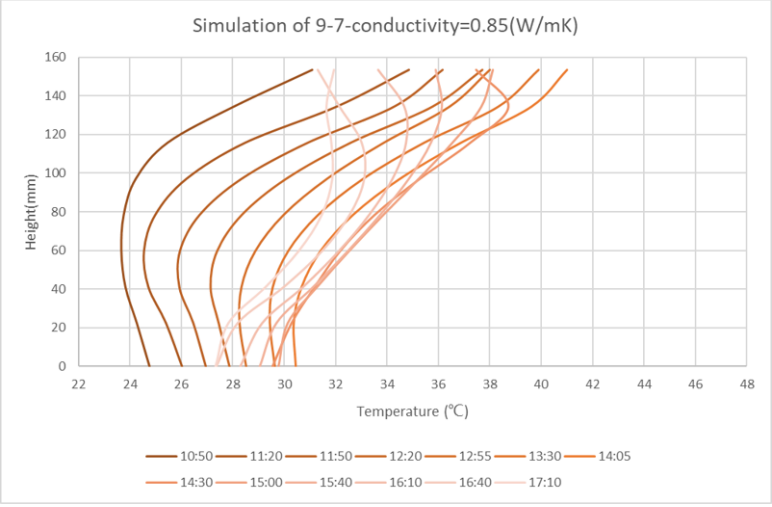

(b) 9-07FEM

Figure 4.19: Comparison of simulation result and experiment for day time on 9-07

ANALYSIS AND COMPARISON

1. **Analysis**
   At the first sight of the results of FEM and experiments, the trend of temperature change is similar: the side surface temperature increases swiftly until 14:30 and decreases slowly between 14:30 to 17:10.

   In the temperature increasing period, both FEM and experiment shows that top surface and bottom surface are heated up faster than middle because the the heat energy needs time to be conducted into the middle of the FRP deck. The results of FEM and experiment both reach the maximum value at around 14:30. According to the irradiance in Figure4.20, the maximum solar irradiance value reaches at 14:00. It can be seen that if the FRP bridge deck's temperature wants to increase continuously over 46.8°C, the irradiance should be more than $700 W/m^2$.

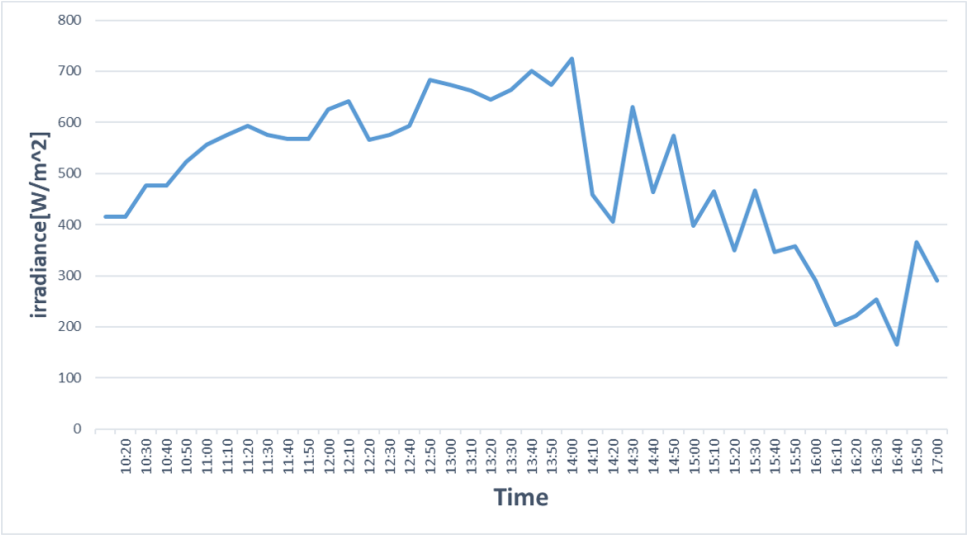

Figure 4.20: Solar irradiance of 9-07

However, the maximum temperature of experiment is 4.92°C higher than that of FEM simulation at 14:30 when the temperature of the specimen reaches maximum. There are two reasons for this deviation:

2. The deviation accumulates with the time and reaches a high value after 230min at 14:30.

3. The environment has natural factors other than solar irradiance like reflection from the buildings which heat up the bridge deck specimen.

In the temperature decreasing period, the middle part temperature decreases about 2°C both in the results of FEM and experiment. The top surface temperature drops about 13°C in experiment while that of FEM only drops about 9°C. This phenomena may also be related to setting of the material property. As for the bottom temperature, both results of FEM and experiment decreases about 4°C.

4. **Quantification of difference**
To quantify the difference between results of FEM and experiment, the temperature difference of web surface at the same height is calculated as:$\Delta T = T_{experiment} - T_{FEM}$. The height of specimen is evenly divided into 9 points and the ΔT of these height are added up as the temperature difference of this time. The temperature difference of different time is shown in Figure4.21. And the absolute values of ΔT are also added up along the height as the absolute temperature difference in Figure4.22.

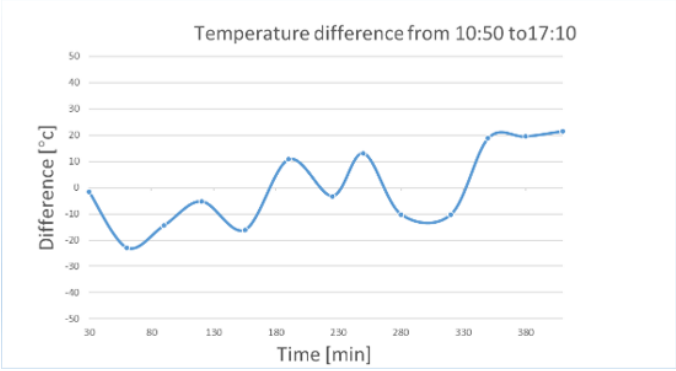

Figure 4.21: Temperature difference of FEM and experiment

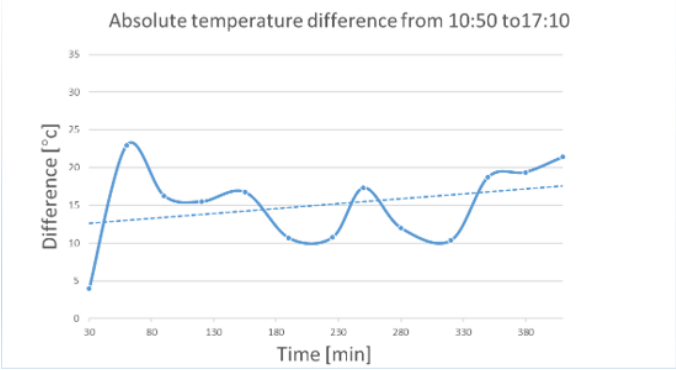

Figure 4.22: Absolute temperature difference of FEM and experiment

Table 4.7: Deviation of FEM and experiment for day time simulation

Time (min)	ΔT	Absolute ΔT
30	-1.72	3.95
60	-22.97	22.97
90	-14.50	16.27
120	-5.33	15.49
155	-16.15	16.75
190	10.69	10.69
225	-3.27	10.74
250	13.00	17.32
280	-10.24	12.01
320	-10.35	10.35
350	18.76	18.76
380	19.40	19.40
410	21.43	21.43

The value of temperature difference shows the entire difference between results of FEM and experiment. Since the value of temperature difference is fluctuating around zero and the amplitude keeps almost the same, the result of FEM could predict the temperature of specimen in a relatively accurate trend. The maximum temperature difference is 21.427°C at the end of day, because the inaccuracy will accumulate with the time. But it only has an average temperature difference of 2.38°C between the FEM result and experiment result.
The value of absolute temperature difference shows the deviation of the detailed part of the temperature plot. Although the entire temperature is relatively accurate in a long time period, the deviation of FEM result with real situation still grows with time slowly. It means the longer the simulation time is, the less accurate the result is. However, the value of maximum absolute temperature difference is 22.97°C at 11:50. This value is abrupt but the main trend of the absolute temperature difference is shown as the dash line of Figure 4.22, still increasing with time.
Generally speaking, an average deviation of 2.38°C and maximum temperature difference at the top surface for 4.92°C is acceptable in a 7h simulation.

Table 4.8: Validation of the day time simulation

	ΔT(°C)	Time
Maximum ΔT	21.427	17:10
Maximum ΔT at top surface	4.92	14:30
Maximum absolute ΔT	21.427	17:10

5

CONCLUSION

First of all, the experiment results tells that the maximum temperature of the FRP bridge deck is capable to reach over 53.9°C in Netherlands, not to mention that the experiment date is not the hottest day of the year. Considering the strength reduction, the prediction of temperature within FRP bridge deck is important and necessary. What's more, the heat from ground reflection is 23% of the solar irradiance, which significantly increase the bottom temperature of the bridge deck. Concluded from the average top temperature change during the day time, solar irradiance is found to be the main factor that determine the maximum temperature of the day because the heat transfers very fast within the FRP material.

The finite element model built in this thesis has an average deviation of 2.38°C and a maximum temperature deviation of 4.92°C, which has only 10.5% deviation compared to experimental data in a 7h simulation during the day. This result is quite acceptable and satisfies the goal set in the beginning of the thesis. Besides, the sensitivity of convection, conductance between FRP and foam, material properties are all studied in this paper. Although there is no available data online for the conductance and convection used in the experiment, appropriate values are found by comparing FEM results to the experimental data.

For convection model, the experience formula used in this thesis is basically right. However, considering the complicated situation of convection, using simplified function which only contains wind speed as variable is more practical and sufficient enough in engineering design. A simplified function for convection model is found as:

$$y = 2.7992V + 12.471$$

For the conductance between FRP and foam, an appropriate value of $2\times10^{-7}W/(mm{\cdot}K)$ is found by comparing the web-core temperature difference between FEM and experiments. In the end an accurate prediction is reached with 21% deviation for the

whole temperature difference along the thickness and 3.5% deviation for the maximum temperature difference along the thickness.

For material properties, the conductivity, density and specific heat capacity of FRP panel all have obvious influence on the temperature of the whole FRP bridge deck. Knowing the exact thermal properties from manufacturing company is the best way but now these properties can rarely be found. Even there is recommended value from the code, it is still not sufficient for engineering design. Take conductivity as example, the only data that could be found in code is get from hot plate method[26] which only detects the conductivity in perpendicular direction of the fiber. However, the FRP panel is an orthotropic composite material which is laid up by sheets of Fiber reinforced polymer, which have different thermal conductivity in perpendicular direction and horizontal direction.
Limited by the equipment and time, the material properties can not be tested by ourselves. But it is still possible to optimize the FEM result by changing the material properties. Taking absolute temperature difference as the controlling parameter, adjust every single material properties until the minimum absolute temperature difference is reached. Although it takes a lot of time manually, it is possible to simplify this process by machine learning.

To be concluded, the Finite element model built in this research has an high accuracy predicting the temperature within the FRP bridge deck. The deviation of prediction is listed in the Table below:

Table 5.1: Deviation of the prediction of FEM

Deviation of maximum temperature difference of web-core	3.5%
Deviation of average temperature difference of web-core	21%
Deviation of maximum temperature of top surface	10.5%
Deviation of average temperature of the FRP web	6%

Finally, this thesis builds a step stone for further researches on the mechanical behavior of FRP deck in elevated temperatures. With the effort of innovative engineers, the promotion of FRP bridges is around the corner.

BIBLIOGRAPHY

[1] P. Kumar, K. Chandrashekhara, and A. Nanni, "Structural performance of a frp bridge deck," Construction and building materials, vol. 18, no. 1, pp. 35–47, 2004.

[2] S. Cao, W. Zhis, and X. Wang, "Tensile properties of cfrp and hybrid frp composites at elevated temperatures," Journal of composite materials, vol. 43, no. 4, pp. 315–330, 2009.

[3] G. Olivier, F. Csillag, E. Tromp, and M. Pavlović, "Static, fatigue and creep performance of blind-bolted connectors in shear experiments on steel-frp joints," Engineering Structures, vol. 230, p. 111713, 2021.

[4] M. N. Ã-zisik, M. N. Özışık, and M. N. Özısık, Heat conduction. John Wiley & Sons, 1993.

[5] J. Fourier, "Théorie analytique de la chaleur (1822)," May 2007. [Online]. Available: https://www.sciencedirect.com/science/article/pii/B9780444508713501078

[6] J. R. Howell, M. P. Mengüç, K. Daun, and R. Siegel, Thermal radiation heat transfer. CRC press, 2020.

[7] A. Bejan, Convection Heat Transfer. John Wiley amp; Sons, 2013.

[8] M. Bahrami, "Forced convection heat transfer," Nov 2022. [Online]. Available: https://www.sfu.ca/~mbahrami/ensc388.html

[9] ——, "Ensc 388 natural convection heat transfer," 2013. [Online]. Available: https://www.sfu.ca/~mbahrami/ensc388.html

[10] I. Cartagenas, "Thermal conductivity of steel," Feb 2022. [Online]. Available: https://thermtest.com/thermal-conductivity-of-steel

[11] K. Kingspan, "Declaration of performance," 2013. [Online]. Available: https://www.kingspan.com/roe/el-gr/products/insulation/declaration-of-performance

[12] "Air - density, specific weight and thermal expansion coefficient vs. temperature and pressure," 2003. [Online]. Available: https://www.engineeringtoolbox.com/air-density-specific-weight-d_600.html

[13] E. Edge, "Viscosity of air, dynamic and kinematic," 2000. [Online]. Available: https://www.engineersedge.com/physics/viscosity_of_air_dynamic_and_kinematic_14483.htm

[14]

[15] P. Bijl, A. Heikkilä, S. Syrjälä, A. Aarva, and A. Poikonen, "Modelling of sample surface temperature in an outdoor weathering test," Polymer testing, vol. 30, no. 5, pp. 485–492, 2011.

[16] T. L. Bergman, T. L. Bergman, F. P. Incropera, D. P. Dewitt, and A. S. Lavine, Fundamentals of heat and mass transfer. John Wiley & Sons, 2011.

[17] R. J. Goldstein and K.-S. Lau, "Laminar natural convection from a horizontal plate and the influence of plate-edge extensions," Journal of Fluid Mechanics, vol. 129, pp. 55–75, 1983.

[18] R. N. M. Institute, "Meteorologisch data portal," 2022. [Online]. Available: https://www.tudelft.nl/?id=59090

[19] F. P. Incropera, D. P. DeWitt, T. L. Bergman, A. S. Lavine et al., Fundamentals of heat and mass transfer. Wiley New York, 1996, vol. 6.

[20] "Foam density, weight, firmness and usability," Jul 2022. [Online]. Available: https://trocellen.com/foam-density/

[21] M. S. Hopkins, Polyurethane foam infill for fiber reinforced polymer (FRP) bridge deck panels: An evaluation of core alternatives using small scale experimental testing. Missouri University of Science and Technology, 2014.

[22] "Surface emissivity – why it matters in insulation," Jul 2016. [Online]. Available: https://www.sigmalabs.com/blog/surface-emissivity-why-it-matters-in-insulation.html

[23] "Pur (flexible foam)," 2016. [Online]. Available: https://designerdata.nl/materials/plastics/foams/polyurethane-flexible-foam

[24] 2022. [Online]. Available: https://gchem.cm.utexas.edu/data/section2.php?target=heat-capacities.php

[25] J. R. Davis, Metals handbook. ASM International, 1998.

[26] S. Akçaözoğlu, K. Akçaözoğlu, and C. D. Atiş, "Thermal conductivity, compressive strength and ultrasonic wave velocity of cementitious composite containing waste pet lightweight aggregate (wpla)," Composites Part B: Engineering, vol. 45, no. 1, pp. 721–726, 2013.

[27] "Understanding the difference between thermal resistance amp; thermal conductance – c-therm technologies ltd.." Aug 2022. [Online]. Available: https://ctherm.com/resources/helpful-links-tools/thermalresistanceandconductivity/

[28] J. K. Page, "Methods for the estimation of solar energy on vertical and inclined surfaces," in Solar Energy Conversion. Elsevier, 1979, pp. 37–99.

[29] P. N. N. ce14b097, "Abaqus/cae user's manual abaqus/cae user's manual," Mar 2019. [Online]. Available: https://www.academia.edu/38631701/ABAQUS_CAE_Users_Manual_ABAQUS_CAE_Users_Manual

[30] D. Zhang, Y. Qin, W. Feng, M. Huang, X. Wang, and S. Yang, "Microstructural evolution of the amorphous layers on mg-zn-ca alloy during laser remelting process," Surface and Coatings Technology, vol. 363, pp. 87–94, 2019.

[31] J. P. Holman, "Heat transfer." 2010.

A

APPENDIX A

```
h=1;
Aconv=0.185;
P=1.74;
Lc=Aconv/P; %characteristic length
V=5; %wind velocity;
v=1.562*(10^-5); %kinematic viscosity
miu=1.85*(10^-5); %dynamic viscosity
Beta=0.0034; %volumetric thermal expansion coefficient;
g=9.8;
Ts=15.7;
Tf=0;
rou=1.184; %density of air
Gr=g*Beta*(rou^2)*(Ts-Tf)*(Lc^3)/(v^2);
%Grasshof number (the ratio of buoyancy forces to viscous forces);
ReL=rou*V*Lc/miu;
%Reynolds number (the ratio of inertia to viscous forces);
Re=rou*V*0.5*Lc/miu;
%Reynolds number at 0.5L length as average
cp=1007; %specific heat of air

k=0.0255; %conductivity of air, 25 degrees
Pr=cp*miu/k; %the Prandtl number

Ra=Gr*Pr;
c=1;
n=1;
Nuforced=0.664*(ReL^(1/2))*(Pr^(1/3));
display(Pr);
display(Gr);
display(ReL);
display(Ra);

```

A

```
33 if (Gr/(Re^2)<0.01)&&(Pr>0.6) %forced convection
34
35     h=Nuforced*k/Lc;
36     display(['forced␣convection␣h=',num2str(h)]);
37
38 end
39 if (Ra>10000000)&&(Ra<10e10)
40     c=0.27;
41     n=0.25;
42 end
43 if (10000<Ra)&&(Ra<10000000) %upper hot lower cold situation
44     c=0.54;
45     n=0.25;
46 end
47 if (2000<Ra)&&(Ra<10000)
48     c=0.38;
49     n=0.25;
50 end
51 if (10<Ra)&&(Ra<2000)
52     c=0.467;
53     n=0.2;
54 end
55 Nufree=c*(Ra^n);
56 if (Gr/(Re^2)>100) %free convection
57
58     h=Nufree*k/Lc;
59     display(['free␣convection␣h=',num2str(h)]);
60
61 end
62 if (Gr/(Re^2)<100)&&(Gr/(Re^2)>0.01)
63     Nu=(Nuforced^(7/2)+Nufree^(7/2))^(2/7);
64     h=Nu*k/Lc;
65     display(['mixed␣convection␣h=',num2str(h)]);
66
67 end
```

B

APPENDIX B

Table B.1: Data processing of temperature of side surface

	Middle		Left		Right	
	Height(mm)	T(°C)	Height(mm)	T(°C)	Height(mm)	T(°C)
1	153.5	39.429	153.5	39.745	153.5	38.301
2	152.58631	39.138	152.58631	39.732	152.59172	40.074
3	151.67262	38.714	151.67262	39.535	151.68343	39.903
4	150.75893	38.14	150.75893	39.178	150.77515	39.455
5	149.84524	37.43	149.84524	38.474	149.86686	38.714
6	148.93155	36.891	148.93155	38.007	148.95858	38.087
7	148.01786	36.457	148.01786	37.725	148.0503	37.672
8	147.10417	35.954	147.10417	37.336	147.14201	37.134
9	146.19048	35.53	146.19048	36.755	146.23373	36.688
10	145.27679	35.201	145.27679	36.158	145.32544	36.144
11	144.3631	34.953	144.3631	35.858	144.41716	35.735
12	143.4494	34.678	143.4494	35.68	143.50888	35.352
13	142.53571	34.249	142.53571	35.283	142.60059	35.118
14	141.62202	33.971	141.62202	34.981	141.69231	34.76
15	140.70833	33.721	140.70833	34.76	140.78402	34.401
16	139.79464	33.33	139.79464	34.373	139.87574	33.985
17	138.88095	32.895	138.88095	33.971	138.96746	33.762
18	137.96726	32.063	137.96726	33.176	138.05917	33.386
19	137.05357	30.896	137.05357	32.29	137.15089	32.937
20	136.13988	30.624	136.13988	31.823	136.2426	31.353
21	135.22619	30.336	135.22619	31.681	135.33432	31.225
22	134.3125	30.221	134.3125	31.467	134.42604	31.096
23	133.39881	30.033	133.39881	31.225	133.51775	31.025
24	132.48512	29.903	132.48512	30.939	132.60947	30.896

B

25	131.57143	29.599	131.57143	30.695	131.70118	30.71
26	130.65774	29.352	130.65774	30.523	130.7929	30.365
27	129.74405	29.221	129.74405	30.278	129.88462	29.932
28	128.83036	29.002	128.83036	30.019	128.97633	29.715
29	127.91667	28.886	127.91667	29.831	128.06805	29.541
30	127.00298	28.666	127.00298	29.657	127.15976	29.236
31	126.08929	28.49	126.08929	29.483	126.25148	29.046
32	125.1756	28.329	125.1756	29.294	125.3432	28.783
33	124.2619	28.197	124.2619	29.119	124.43491	28.652
34	123.34821	28.035	123.34821	28.929	123.52663	28.549
35	122.43452	27.976	122.43452	28.739	122.61834	28.461
36	121.52083	27.887	121.52083	28.578	121.71006	28.329
37	120.60714	27.784	120.60714	28.476	120.80178	28.167
38	119.69345	27.651	119.69345	28.27	119.89349	28.05
39	118.77976	27.577	118.77976	28.153	118.98521	27.976
40	117.86607	27.503	117.86607	28.094	118.07692	27.917
41	116.95238	27.414	116.95238	27.932	117.16864	27.858
42	116.03869	27.355	116.03869	27.814	116.26036	27.814
43	115.125	27.266	115.125	27.74	115.35207	27.769
44	114.21131	27.191	114.21131	27.636	114.44379	27.725
45	113.29762	27.147	113.29762	27.547	113.5355	27.695
46	112.38393	27.102	112.38393	27.503	112.62722	27.725
47	111.47024	27.043	111.47024	27.37	111.71893	27.74
48	110.55655	26.953	110.55655	27.295	110.81065	27.725
49	109.64286	26.879	109.64286	27.206	109.90237	27.681
50	108.72917	26.819	108.72917	27.132	108.99408	27.636
51	107.81548	26.745	107.81548	27.087	108.0858	27.592
52	106.90179	26.7	106.90179	27.043	107.17751	27.399
53	105.9881	26.685	105.9881	26.968	106.26923	27.162
54	105.0744	26.655	105.0744	26.924	105.36095	27.043
55	104.16071	26.61	104.16071	26.864	104.45266	26.968
56	103.24702	26.55	103.24702	26.804	103.54438	26.968
57	102.33333	26.505	102.33333	26.745	102.63609	26.968
58	101.41964	26.461	101.41964	26.715	101.72781	26.968
59	100.50595	26.416	100.50595	26.67	100.81953	26.953
60	99.592262	26.371	99.592262	26.61	99.911243	26.924
61	98.678571	26.341	98.678571	26.565	99.002959	26.894
62	97.764881	26.311	97.764881	26.55	98.094675	26.849
63	96.85119	26.296	96.85119	26.52	97.186391	26.804
64	95.9375	26.281	95.9375	26.505	96.278107	26.759
65	95.02381	26.266	95.02381	26.49	95.369822	26.745
66	94.110119	26.236	94.110119	26.476	94.461538	26.7
67	93.196429	26.206	93.196429	26.446	93.553254	26.685
68	92.282738	26.176	92.282738	26.431	92.64497	26.67
69	91.369048	26.146	91.369048	26.416	91.736686	26.655

70	90.455357	26.146	90.455357	26.416	90.828402	26.625
71	89.541667	26.131	89.541667	26.401	89.920118	26.61
72	88.627976	26.131	88.627976	26.401	89.011834	26.595
73	87.714286	26.131	87.714286	26.401	88.10355	26.58
74	86.800595	26.116	86.800595	26.371	87.195266	26.565
75	85.886905	26.101	85.886905	26.386	86.286982	26.55
76	84.973214	26.086	84.973214	26.386	85.378698	26.52
77	84.059524	26.071	84.059524	26.371	84.470414	26.49
78	83.145833	26.071	83.145833	26.371	83.56213	26.461
79	82.232143	26.055	82.232143	26.341	82.653846	26.416
80	81.318452	26.055	81.318452	26.311	81.745562	26.386
81	80.404762	26.04	80.404762	26.311	80.837278	26.371
82	79.491071	26.04	79.491071	26.296	79.928994	26.356
83	78.577381	26.04	78.577381	26.326	79.02071	26.371
84	77.66369	26.025	77.66369	26.326	78.112426	26.401
85	76.75	26.04	76.75	26.341	77.204142	26.416
86	75.83631	26.025	75.83631	26.356	76.295858	26.416
87	74.922619	26.025	74.922619	26.356	75.387574	26.416
88	74.008929	26.025	74.008929	26.341	74.47929	26.416
89	73.095238	26.04	73.095238	26.326	73.571006	26.401
90	72.181548	26.04	72.181548	26.311	72.662722	26.401
91	71.267857	26.04	71.267857	26.296	71.754438	26.416
92	70.354167	26.055	70.354167	26.281	70.846154	26.401
93	69.440476	26.025	69.440476	26.266	69.93787	26.371
94	68.526786	26.025	68.526786	26.311	69.029586	26.341
95	67.613095	25.995	67.613095	26.326	68.121302	26.311
96	66.699405	26.01	66.699405	26.311	67.213018	26.281
97	65.785714	25.995	65.785714	26.311	66.304734	26.281
98	64.872024	25.995	64.872024	26.311	65.39645	26.311
99	63.958333	25.995	63.958333	26.326	64.488166	26.356
100	63.044643	25.98	63.044643	26.341	63.579882	26.386
101	62.130952	25.98	62.130952	26.356	62.671598	26.401
102	61.217262	25.98	61.217262	26.371	61.763314	26.431
103	60.303571	26.01	60.303571	26.401	60.85503	26.431
104	59.389881	25.965	59.389881	26.446	59.946746	26.446
105	58.47619	25.95	58.47619	26.461	59.038462	26.446
106	57.5625	25.935	57.5625	26.49	58.130178	26.446
107	56.64881	25.95	56.64881	26.52	57.221893	26.446
108	55.735119	25.98	55.735119	26.535	56.313609	26.446
109	54.821429	26.01	54.821429	26.58	55.405325	26.446
110	53.907738	26.01	53.907738	26.61	54.497041	26.476
111	52.994048	26.04	52.994048	26.625	53.588757	26.49
112	52.080357	26.04	52.080357	26.655	52.680473	26.461
113	51.166667	26.025	51.166667	26.655	51.772189	26.461
114	50.252976	26.01	50.252976	26.655	50.863905	26.49

B

115	49.339286	25.995	49.339286	26.655	49.955621	26.505
116	48.425595	26.01	48.425595	26.67	49.047337	26.52
117	47.511905	26.01	47.511905	26.7	48.139053	26.52
118	46.598214	26.025	46.598214	26.745	47.230769	26.52
119	45.684524	26.025	45.684524	26.774	46.322485	26.52
120	44.770833	26.04	44.770833	26.819	45.414201	26.535
121	43.857143	26.04	43.857143	26.849	44.505917	26.55
122	42.943452	26.055	42.943452	26.879	43.597633	26.58
123	42.029762	26.071	42.029762	26.924	42.689349	26.595
124	41.116071	26.101	41.116071	26.938	41.781065	26.61
125	40.202381	26.131	40.202381	26.953	40.872781	26.625
126	39.28869	26.161	39.28869	26.998	39.964497	26.64
127	38.375	26.221	38.375	27.028	39.056213	26.64
128	37.46131	26.266	37.46131	27.087	38.147929	26.64
129	36.547619	26.281	36.547619	27.147	37.239645	26.655
130	35.633929	26.326	35.633929	27.191	36.331361	26.685
131	34.720238	26.341	34.720238	27.251	35.423077	26.73
132	33.806548	26.356	33.806548	27.31	34.514793	26.789
133	32.892857	26.386	32.892857	27.34	33.606509	26.834
134	31.979167	26.401	31.979167	27.384	32.698225	26.864
135	31.065476	26.416	31.065476	27.444	31.789941	26.894
136	30.151786	26.461	30.151786	27.503	30.881657	26.924
137	29.238095	26.505	29.238095	27.562	29.973373	26.968
138	28.324405	26.565	28.324405	27.651	29.065089	27.028
139	27.410714	26.625	27.410714	27.725	28.156805	27.072
140	26.497024	26.685	26.497024	27.784	27.248521	27.102
141	25.583333	26.73	25.583333	27.843	26.340237	27.162
142	24.669643	26.789	24.669643	27.917	25.431953	27.251
143	23.755952	26.864	23.755952	28.005	24.523669	27.325
144	22.842262	26.938	22.842262	28.02	23.615385	27.429
145	21.928571	27.087	21.928571	28.05	22.707101	27.473
146	21.014881	27.28	21.014881	28.123	21.798817	27.577
147	20.10119	27.34	20.10119	28.182	20.890533	27.636
148	19.1875	27.399	19.1875	28.241	19.982249	27.695
149	18.27381	27.414	18.27381	28.3	19.073964	27.769
150	17.360119	27.429	17.360119	28.373	18.16568	27.799
151	16.446429	27.458	16.446429	28.578	17.257396	27.843
152	15.532738	27.488	15.532738	28.666	16.349112	27.873
153	14.619048	27.562	14.619048	28.856	15.440828	27.902
154	13.705357	27.621	13.705357	28.915	14.532544	27.976
155	12.791667	27.636	12.791667	29.061	13.62426	28.02
156	11.877976	27.695	11.877976	29.148	12.715976	28.123
157	10.964286	27.769	10.964286	29.25	11.807692	28.27
158	10.050595	27.828	10.050595	29.425	10.899408	28.373
159	9.1369048	27.932	9.1369048	29.483	9.9911243	28.446

160	8.2232143	28.05	8.2232143	29.642	9.0828402	28.534
161	7.3095238	28.197	7.3095238	29.744	8.1745562	28.564
162	6.3958333	28.3	6.3958333	29.946	7.2662722	28.725
163	5.4821429	28.461	5.4821429	30.12	6.3579882	28.915
164	4.5684524	28.622	4.5684524	30.235	5.4497041	29.075
165	3.6547619	28.71	3.6547619	30.379	4.5414201	29.148
166	2.7410714	28.798	2.7410714	30.552	3.6331361	29.41
167	1.827381	28.856	1.827381	30.724	2.7248521	29.729
168	0.9136905	28.944	0.9136905	30.896	1.816568	29.874
169					0.908284	29.975